

GREAT SALT LAKE'S NORTH ARM SALT CRUST

by Andrew Rupke, Taylor Boden, and Peter Nielsen



REPORT OF INVESTIGATION 276
UTAH GEOLOGICAL SURVEY
a division of
UTAH DEPARTMENT OF NATURAL RESOURCES
2016

GREAT SALT LAKE'S NORTH ARM SALT CRUST

by Andrew Rupke, Taylor Boden, and Peter Nielsen

ISBN: 978-1-55791-932-8

Cover photo: Exposed salt crust on the west side of the north arm of Great Salt Lake.



REPORT OF INVESTIGATION 276

UTAH GEOLOGICAL SURVEY

a division of

UTAH DEPARTMENT OF NATURAL RESOURCES

2016

STATE OF UTAH

Gary R. Herbert, Governor

DEPARTMENT OF NATURAL RESOURCES

Michael Styler, Executive Director

UTAH GEOLOGICAL SURVEY

Richard G. Allis, Director

PUBLICATIONS

contact

Natural Resources Map & Bookstore

1594 W. North Temple

Salt Lake City, UT 84116

telephone: 801-537-3320

toll-free: 1-888-UTAH MAP

website: mapstore.utah.gov

email: geostore@utah.gov

UTAH GEOLOGICAL SURVEY

contact

1594 W. North Temple, Suite 3110

Salt Lake City, UT 84116

telephone: 801-537-3300

website: geology.utah.gov

Although this product represents the work of professional scientists, the Utah Department of Natural Resources, Utah Geological Survey, makes no warranty, expressed or implied, regarding its suitability for a particular use. The Utah Department of Natural Resources, Utah Geological Survey, shall not be liable under any circumstances for any direct, indirect, special, incidental, or consequential damages with respect to claims by users of this product. The Utah Geological Survey does not endorse any products or manufacturers. Reference to any specific commercial product, process, service, or company by trade name, trademark, or otherwise, does not constitute endorsement or recommendation by the Utah Geological Survey.

CONTENTS

ABSTRACT.....	1
INTRODUCTION	1
Background and Purpose	1
Previous Work.....	3
Methods.....	3
General	3
Access	3
Thickness measurements	3
Salt crust sampling.....	4
Salt crust mapping.....	5
Analytical methods	5
NORTH ARM SALT CRUST.....	5
Description.....	5
Chemistry and Mineralogy	10
Thickness	12
North Arm Precipitated Salt Load.....	17
CONSIDERATIONS FOR FUTURE STUDY.....	20
CONCLUSIONS.....	21
ACKNOWLEDGMENTS	21
REFERENCES	22
APPENDICES	23
Appendix A—Goodwin (1973a) report summary	25
Appendix B—Supplementary photographs	35
Appendix C—Sample data	44
Appendix D—Salt crust thickness measurement data.....	46

FIGURES

Figure 1. Transect locations around the north arm of Great Salt Lake.....	2
Figure 2. Salt crust drilling with rotary hammer and masonry bit.....	4
Figure 3. Coarsely crystalline halite from north arm salt crust.....	5
Figure 4. Extent of the north arm salt crust in August 2014.....	6
Figure 5. Zone of salt crust dissolution.....	7
Figure 6. Salt isopach map from Goodwin (1973a).....	7
Figure 7. Amoco Production Company borehole locations and salt thickness.....	8
Figure 8. In-place, submerged crystalline halite.....	8
Figure 9. Smooth, crystalline salt crust exposed above water level	8
Figure 10. Channel where runoff has dissolved the salt crust	9
Figure 11. Accumulations of salt rafts	9
Figure 12. Photomicrograph of halite crystals in the salt crust showing both euhedral and subhedral faces.....	9
Figure 13. Photomicrograph of large, subhedral crystals	10
Figure 14. Photomicrograph of layered halite crystals	10
Figure 15. Thin section showing crystal-supported matrix and pore space.....	10
Figure 16. Photomicrographs of halite and gypsum crystals.....	10
Figure 17. Transect 1 with salt crust thickness in feet.....	13
Figure 18. Transect 2 with salt crust thickness in feet.....	13
Figure 19. Transect 3 with salt crust thickness in feet.....	14
Figure 20. Transect 4 with salt crust thickness in feet.....	14
Figure 21. Transect 5 with salt crust thickness in feet.....	15
Figure 22. Transect 6 with salt crust thickness in feet.....	15
Figure 23. Transect 7 with salt crust thickness in feet.....	16
Figure 24. Transect 8 with salt crust thickness in feet.....	16
Figure 25. Transect 9 with salt crust thickness in feet.....	17

Figure 26. Salt isopach map.....	18
Figure 27. The water's edge near Spiral Jetty.....	19
Figure 28. Estimates of the precipitated salt load in the north arm of Great Salt Lake from 1963 through 2015.....	21

TABLES

Table 1. Chemical composition of the salt crust.....	11
Table 2. Chemical composition of the salt crust as determined by previous studies.....	11
Table 3. Thickness measurements of the salt crust from previous studies	12
Table 4. Salt gauge data from Hahl and Handy (1969).....	20
Table 5. Tonnage estimates of precipitated salt in the north arm of Great Salt Lake from previous studies.....	20

PLATE

Plate 1. North arm salt crust map and thickness data

GREAT SALT LAKE'S NORTH ARM SALT CRUST

by Andrew Rupke, Taylor Boden, and Peter Nielsen

ABSTRACT

The rock-fill railroad causeway that separates the north and south arms of Great Salt Lake restricts the flow of brine throughout the lake causing the north arm, also known as Gunnison Bay, to be much more saline than other areas. The causeway was completed in 1959, and for much of the time since then, the north arm's salinity levels have been high enough to cause precipitation of a salt crust on the floor of that part of the lake. Past estimates suggest that, at times, 20% or more of the total salt load of Great Salt Lake has been sequestered in the north arm's salt crust. Research focusing on the salt crust has been limited with the exception of a Utah Geological and Mineralogical Survey study completed during the early 1970s that was never published. Although limited, previous data indicate that the salt crust is primarily halite and can reach thicknesses of up to 8 feet towards central parts of the north arm. A comprehensive review and evaluation of previous data suggest that the most robust estimate of the precipitated salt load (about 1.1 billion short tons—from the unpublished study) may be low. Most recently (and more commonly), the precipitated salt load of the lake has been calculated indirectly for a range of time, based on dissolved solids content of the lake brine; however, the maximum estimate of precipitated salt load by this method for any time since completion of the causeway is below 1 billion short tons.

We investigated the north arm salt crust along nine nearshore transects around the north arm during late 2015 and early 2016 and encountered a competent salt crust at each transect. Our results from examination of the crust, chemical analysis, and x-ray diffraction confirm that the crust is almost entirely halite. Detailed orthophotographic mapping indicates that the salt crust covered an area of about 414 square miles during August 2014. We measured crust thickness along these transects, and our maximum measured thickness reached nearly 1.9 feet. The measurements from late 2015 consistently showed crust thickness of 1 foot (or nearly 1 foot) a short distance into the lake from the water's edge. With this observation, we constructed a 1-foot isopach around the north arm that encloses an area of about 349 square miles. Using the mapped crust and isopach, we estimate a minimum precipitated salt load of 456 million short tons in the north arm of Great Salt Lake during late 2015. The actual precipitated salt load is undoubtedly much higher considering that we measured nearly 1.9 feet of salt on one nearshore transect and that previous data indicate potential for greater thicknesses in central parts of the bay. Although we do not have recent data from the central parts of the north arm, current low lake levels and a comparison of our nearshore data pattern

to previous data with broader coverage allow the possibility for a precipitated salt load in excess of 1 billion short tons for 2015. Because the salt crust is an important component of the lake's salinity cycle, our uncertainty and the potential for significant tonnages of precipitated salt in the north arm highlight the need for additional work. We intend to use our measurements as baseline information for future monitoring of the crust. Monitoring will contribute to our understanding of the crust and how changes in the lake, such as surface level changes, seasonal changes, or causeway modifications, affect the crust.

INTRODUCTION

Background and Purpose

Great Salt Lake (GSL) is a terminal lake for a drainage basin that encompasses much of north-central Utah and adjoining portions of southwestern Wyoming and southeastern Idaho, and it is fed primarily by three major rivers (Bear, Weber, and Jordan). Shortly after the construction of the rock-fill railroad causeway in 1959, that separates Gunnison Bay (the north arm of GSL) and Gilbert Bay (the south arm of GSL), changes in the salinity system of GSL were observed (Adams, 1964) (figure 1). A net movement of dissolved solids to the north of the causeway was identified as salinity levels in the north arm became measurably higher than salinity levels in the south arm (Adams, 1964; Madison, 1970). The salinity difference is a result of nearly all of the freshwater inflow into GSL entering into the south arm and restricted brine flow through the causeway. For much of the recent past, with the exception of the late 1980s and early 1990s, the north arm has been at or near saturation with respect to salt (halite/sodium chloride) (Utah Geological Survey, 2016), and a salt crust has precipitated on the floor of the lake north of the causeway (Loving and others, 2000; Mohammed and Tarboton, 2012).

The salt crust in the north arm is a significant phenomenon because it functions as a salt sink (or reservoir) affecting the overall salinity of GSL. As salt precipitates and is sequestered in the crust, the overall dissolved salt load of the entire lake brine decreases, and the opposite occurs during periods when the salt crust is dissolving. Because a variety of the lake's resources (brine shrimp, mineral industry, and others) are affected by salinity levels, an understanding of the salt crust is important. Previous estimates suggest that about 20% or more of the total salt load of the lake has been sequestered at times in the salt crust of the north arm, but the amount

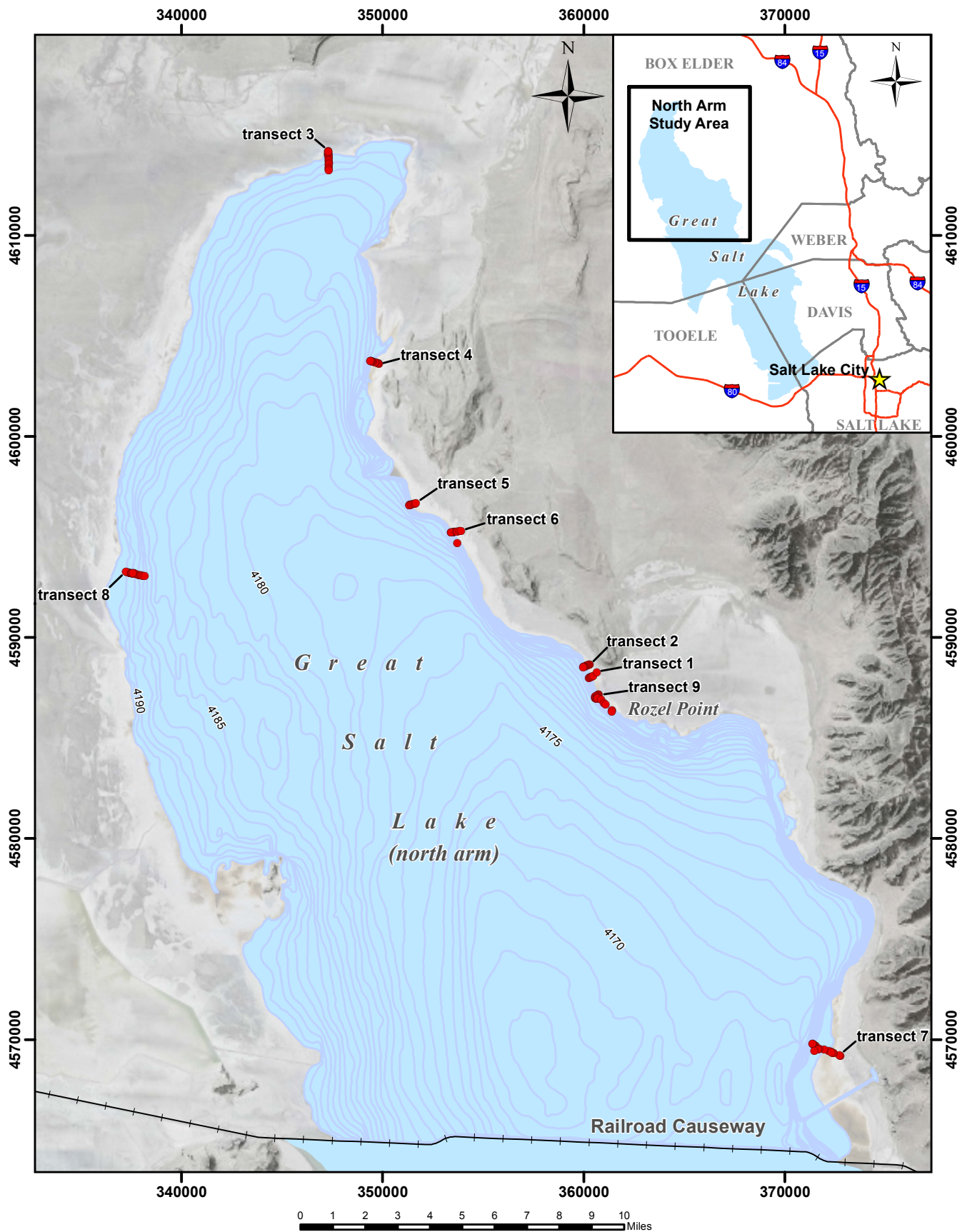


Figure 1. Transect locations (red points) around the north arm of Great Salt Lake. Lake extent (light blue) is shown at 4192 ft elevation. Blue lines represent one-foot contour bathymetry (feet above mean sea level) from Baskin and Turner (2006). Grid coordinates are UTM Z12 NAD83.

fluctuates based on lake conditions (Adams, 1964; Eardley, 1966; Goodwin, 1973a; Loving and others, 2000; Mohammed and Tarboton, 2012). Despite the significant role the salt crust plays in affecting the overall salinity of the lake, past research focusing on the salt crust is limited. The primary objective of this study was to provide some basic information on the salt crust by (1) measuring the thickness of the salt crust at accessible (nearshore) locations, (2) examining the physical and chemical characteristics of the salt crust, (3) mapping the outer extent of the salt crust, and (4) compiling existing data on the salt crust. Additional objectives were to place minimum constraints on the magnitude of sequestered salt through direct measurements and provide baseline data that can be used to detect trends in the precipitated salt load over time.

Previous Work

Goodwin (1973a) provided the most comprehensive information available on the north arm salt crust, but the report and related data are not published or broadly available. The data presented by Goodwin (1973a) are based on several cores of salt crust taken by the Utah Geological Survey (UGS) (at the time, the Utah Geological and Mineralogical Survey [UGMS]) in 1970 and 1972. The report includes basic descriptions of the salt crust, chemical and mineralogical information, thickness data, and a tonnage estimate. Goodwin (1973a) also prepared an isopach map of the salt crust based on the UGMS coring data. Unfortunately, we have not located a final version of this report, and some of the data are incomplete and unclear. Some of Goodwin's (1973a) data are presented in the main body of this report; the report and remaining data are presented in appendix A. Although the original report was not published, Goodwin (1973b) did publish an abstract from his work.

With the exception of Goodwin's (1973a) report, no known research investigations have focused on the salt crust in the north arm of Great Salt Lake. However, a number of publications or reports have provided relevant information on the crust, although the data are limited and often general in nature. Adams' (1964) report was probably the earliest publication to provide information on thickness of the salt crust, estimate the quantity of precipitated salt, and comment on the composition of the salt crust. Handy and Hahl (1966) included a few observations of the salt crust, including thickness, and presented a chemical analysis of the crust. The same year, Cohenour (1966) published a few notes on the tonnage, extent, and thickness of the crust. Hahl and Handy (1969) presented a slightly more detailed description of the crust than previous publications and included some thickness and compositional data. They also presented some gauge data showing rates of accumulation and loss for the salt crust over a two-year period. Eardley (1966, 1970) made limited reference to the north arm salt crust. Hedberg (1970) published a short, page-long article focusing on the salt crust thickness, composition, and

tonnage data. Amoco Production Company completed a few boreholes as part of a geotechnical investigation across GSL in 1974 and 1975. Three holes were completed in the north arm of GSL, and drill logs from Dames and Moore (undated) and a publication from Woodhall (1980) include information from this program. Woodhall (1980) included a brief description of the salt crust cored during this program. Some of the data from these publications are conveyed in later sections of this report.

Many references have taken precipitated salt, including the north arm salt crust, into account when evaluating the salt balance of GSL such as Waddell and Bolke (1973), Whelan (1973), Whelan and Petersen (1975), and Waddell and Fields (1977). Waddell and Bolke (1973) and Waddell and Fields (1977) also reported Goodwin's (1973a) unpublished estimates of the precipitated salt load in the north arm. More recent publications by Wold and others (1997), Loving and others (2000), and Mohammed and Tarboton (2012) projected the tonnage of precipitated salt in the overall GSL system for a wide range of years based on dissolved solids information.

Methods

General

This project began with a search of relevant literature and an examination of aerial photography, but most of the study is a result of field investigations of the salt crust near and along nine transects around the north arm of GSL. The general field area and locations of transects are shown on figure 1. Additional details of our methods relating to specific aspects of the project are described below.

Access

Accessible areas of the salt crust are limited due to extensive mudflats, limited road access, and property restrictions. The most accessible areas of salt crust are on the east side of Gunnison Bay; however, more property restrictions exist on the east side as well. We were able to access multiple points along the east side with an access agreement. Good road access is available to the edge of the mudflats on the north and west sides of Gunnison Bay, but the mudflats are extensive in those areas, particularly on the west side. Currently, mudflats from about 4 to 8 miles wide separate road access and the salt crust along the west side of the north arm. Our only transect on the west side of the bay was reached via helicopter.

Thickness Measurements

We measured salt crust thickness along several shore-perpendicular transects (figure 1 and plate 1). We began each transect at the outer edge of the salt crust, measured crust thickness at several points along each transect, and complet-

ed each transect when the water became too deep to measure the crust. Thickness of the salt crust was determined by drilling vertical holes into the salt crust and using a caliper that we fabricated for this project. We drilled the holes using a cordless rotary hammer with a 37-inch-long, $\frac{3}{4}$ -inch-diameter masonry drill bit. If we needed additional drilling length through water we used an 18-inch extension. Details of the equipment are provided in appendix B. After drilling the hole, we measured the thickness of the salt crust using the caliper. We used the bottom end of the caliper to hook the base of the salt crust, and we then slid the upper part of the caliper into place on the top of the salt. After removing the caliper from the hole, we measured the distance between the ends. We measured crust thickness to the closest $\frac{1}{8}$ of an inch (roughly equivalent to a hundredth of a foot). Typically, one or two holes were drilled at each measurement location and two or more measurements were taken in each hole. If two or more holes were drilled, we generally spaced them less than 1 foot apart. For each location we used all the measurements to calculate an average thickness.

The described method works because there is a dramatic contrast between the salt crust and the substrate which generally consists of a combination of oolitic sand, silt, and mud (figure 2). The salt crust is generally white to light-pink, competent, and consolidated, whereas the substrate is dark gray, fine grained, unconsolidated, and soft with an almost soupy consistency due to saturation. The bottom end of the caliper was used as a probe to some degree to determine if any thin oolitic mud lenses occurred within the salt crust. We periodically drilled as deep as possible to determine if any salt lenses occurred below the first significant oolitic mud interval. In all cases, drilling revealed no discernable salt lenses beneath significant thickness of oolitic sand and mud. The length of each transect was limited to brine depths in which we could make measurements from a logistical standpoint, which was between 2 and 2.5 feet (ft). We noted at each site whether the measurement was taken on land or in the lake.

To estimate the accuracy of this method, we measured several holes using the caliper in a $\frac{3}{4}$ -inch hole and then excavated an area at the same location to more directly observe the thickness. After excavation, measurements indicated that our caliper method was either equivalent to or slightly less than measurements taken from the excavation. Sources of error and variability in our method include roughness of the top or bottom of the salt crust surface and potential breakage at the base of the salt crust that could occur during drilling resulting in an uneven measuring surface. The average standard deviation for most measurement sites is ± 0.02 ft, but for individual sites ranged up to 0.07 ft. In areas where microbialite mounds are prevalent below the salt crust the average standard deviation was significantly higher (0.06 ft) and ranged up to 0.12 ft for individual sites. The location for each measurement site was recorded using a handheld GPS with Wide Area Augmentation System (WAAS) correction to improve accuracy, which we estimate was about 10 ft horizontally. The method



Figure 2. Salt crust drilling with rotary hammer and masonry bit. Drilling through the salt crust yields fine, white cuttings (top). Dark gray cuttings consisting of oolitic sand, silt, and mud are brought to the surface after drilling through the salt crust (bottom). The drill bit diameter is $\frac{3}{4}$ inch.

for measuring thickness was partly driven by the desire to develop an inexpensive measurement method to promote longer term monitoring of the crust. Total cost for our measurement gear (excluding GPS) was approximately \$1000.

Salt Crust Sampling

We sampled blocks of salt crust by drilling several $\frac{3}{4}$ -inch diameter holes around the edge of a block and using a thin, long hand saw to cut the salt in between holes. We then used a shovel or mattock to help pry the samples out. The samples were collected above the water's edge, and sampling photographs can be viewed in appendix B. The sample blocks were cut into vertical slabs to examine the interior and provide material for analytical testing and thin sections. Brine from the sample blocks was allowed to drain for several weeks prior to chemical and mineralogical analyses to reduce the amount of mineral precipitation in the pore space of the samples.

We attempted to sample the salt crust using two coring bits with the rotary hammer, but had no success. The core drill bit did not cut well and would not advance through the salt, which may be due to lack of a method to flush drill cuttings from the hole. However, a “toothier” core bit might have more success extracting a core sample in the future.

We submitted portions of the salt crust to Wagner Petrographic for preparation of thin sections. The samples were vacuum impregnated with blue epoxy to provide added strength for preparation and to show pore space. Because of the soluble nature of the salt, special preparatory techniques were required to create the thin sections.

Salt Crust Mapping

We mapped the outer extent of the salt crust using recent high-resolution orthophotography from Google that was supplied by the Utah Automated Geographic Reference Center (AGRC). The resolution is 6 inches per pixel and nearly all of the photography for the north arm of GSL is from August 17, 2014, with a very small area in the southwest corner dated June 6, 2013. In the photography, the salt crust stands out as bright white, but is patchy in some areas. In other areas a transitional color change exists from white salt crust to gray- and brown-colored mud flat. In our mapping, we attempted to differentiate the patchy and transitional areas from what we interpreted as solid, continuous salt crust. We calibrated our mapping, to some degree, with our fieldwork, but, due to heavy rains during the spring of 2015, some dissolution of the salt crust occurred and an exact comparison was not possible.

Analytical Methods

Chemical analyses were provided by a commercial laboratory that was selected based on its past experience analyzing evaporites. The lab used inductively coupled plasma (ICP) mass spectroscopy to analyze most of the reported elements. X-ray diffraction (XRD) analysis of samples was completed at the UGS using a Rigaku MiniFlex 2 detector. We used Rigaku's PDXL version 2 software to process the XRD spectra and identify mineral diffraction patterns.

NORTH ARM SALT CRUST

Description

The salt crust covering the lake bed of the north arm of GSL is generally composed of white to light pink, coarsely crystalline halite (NaCl). Chemical and mineralogical analyses from this and past studies confirm that the crust is almost completely halite, and more detailed information on chemistry and mineralogy is presented in the next section. The salt crust we examined is mostly composed of halite crystals ranging in size from about 0.04 to 0.5 in (figure 3), which is

consistent with Goodwin's (1973a) and Woodhall's (1980) descriptions. The crust is generally consolidated but brittle. We were able to extract large, intact sample blocks of the crust—pieces could be broken off relatively easily with a hammer, but the samples were solid enough to cut into competent slabs (appendix B). Goodwin (1973a) measured the bulk density of the salt crust from cores, and the results ranged from 0.612 g/cm³ to 1.684 g/cm³. Goodwin's (1973a) calculated mean of 17 measurements was 1.436 g/cm³ with a standard deviation of 0.181 g/cm³. Whelan (1973) used a specific gravity of 1.38 to calculate the tonnage of precipitated salt in the north arm. These estimates of density and specific gravity imply over 30% porosity in the salt crust because solid halite has a specific gravity of 2.16 (Klein and Hurlbut, 1993).

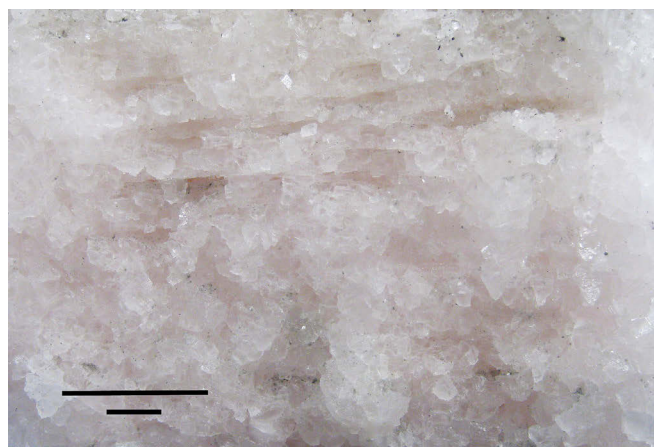


Figure 3. Coarsely crystalline halite from the north arm salt crust. Sample SCI 1 collected on transect 2. Sub-horizontal linear features in upper half of sample likely represent accumulations of salt rafts that have been assimilated into the salt crust. Top black line is 1 inch and lower line is 1 cm.

Evidence indicates that the whole of the submerged and near-shore exposed lake bed north of the causeway is covered by salt crust. Recent orthophotography shows a consistent salt crust surrounding the north arm (figure 4, plate 1), and we observed salt crust at all the sites we visited. Based on our orthophotographic mapping, we estimate that the area of solid salt crust that covered the north arm in August 2014 was about 414 square miles and areas partially covered by salt crust were about 52 square miles. The largest areas of partial crust are on the west side of the lake where the lakebed gradient is low. Small areas of dissolution, likely caused by upwelling of fresh(er) groundwater, are present (figure 5), but our observations suggest that these areas are minimal. Goodwin's (1973a) boreholes across the north arm consistently encountered significant thicknesses of salt (figure 6), and drilling by Amoco (reported in Dames and Moore [undated] and Woodhall [1980]) also showed significant salt in central parts of the north arm (figure 7). Anecdotally, we have noted that while sampling brine for another study, a weighted sample screen lowered from the side of a boat encounters a solid surface at the bottom of the lake in the north arm in contrast to soft sediments encountered in the south arm.

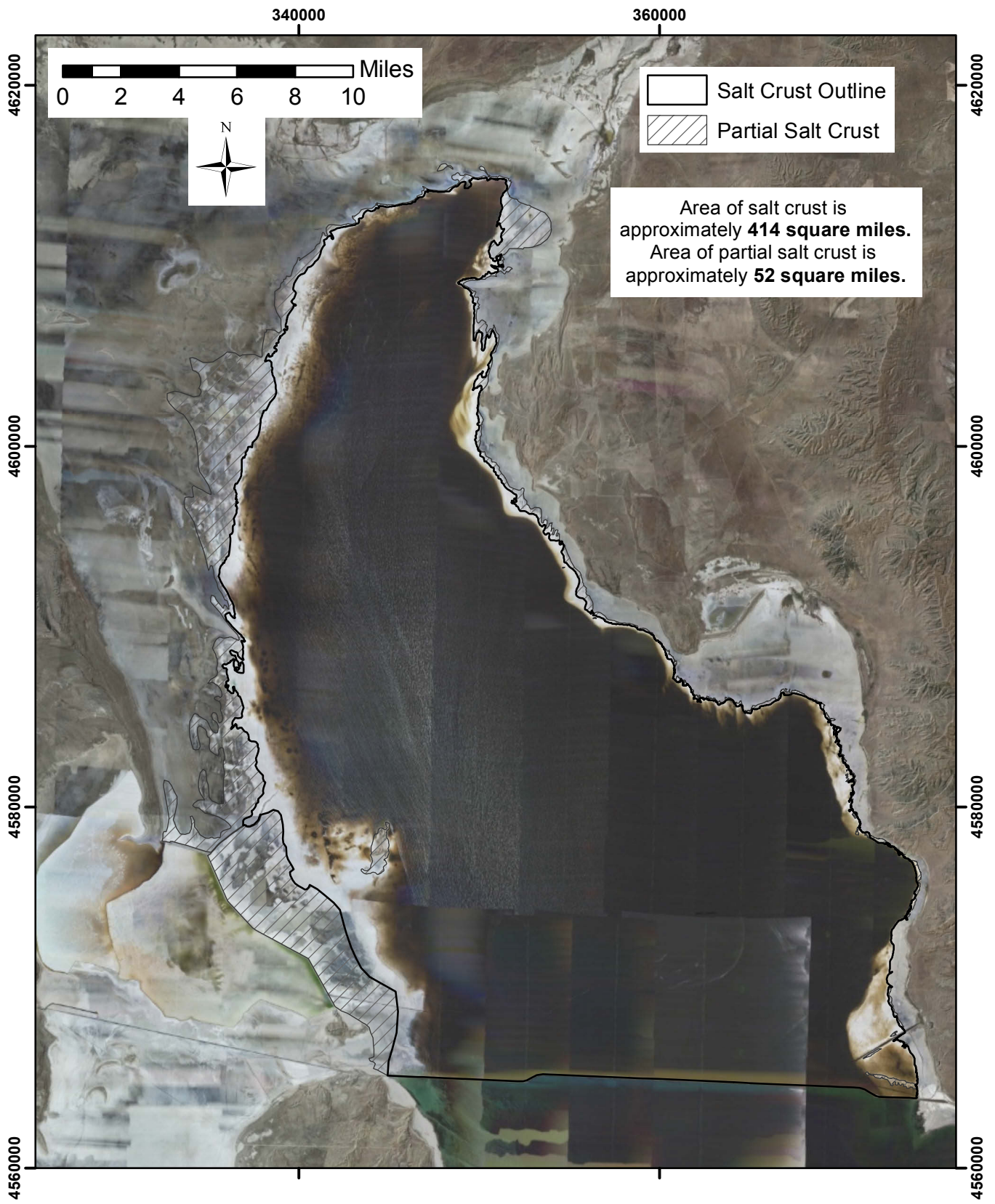


Figure 4. Extent of the north arm salt crust in August 2014. Orthophotographic imagery provided by Google. Imagery discrepancy in the south area is from photography of a different date. Grid coordinates are UTM Z12 NAD83.



Figure 5. Zone of salt crust dissolution. Small, scattered solution holes are likely caused by upwelling of fresher groundwater. Zones of upwelling like this are frequently coincident with microbialite mounds. Photograph from the west side of the north arm along transect 8.

The salt crust can be broadly divided into exposed and submerged areas. Exposed areas are generally being dissolved and submerged areas experience both growth and dissolution, likely seasonally. During late summer and fall when we did most of our field work, the surface of the submerged crust was generally rough in nature due to sharp edges of coarse cubic, halite crystals attached to the lake bed (figure 8). The character of the exposed portion of the crust is variable. In many areas, the crust is smooth and flat and exposes a weathered, pink surface of coarsely crystalline halite (figure 9). Near the water's edge, the exposed salt crust surface tends to have a white, powdery, and granular appearance. This appearance may be the result of wave action causing abrasion of the salt and precipitation of new, fine-grained crystals as water evaporates from the surface of the crust. The exposed salt crust is also dissolved and dissected in many areas from rainfall events, but in some cases those dissected areas have been filled in by salt precipitating from ponded brine (figure 10). In other areas, ponded water, likely from rain events, has created “slushy” zones of unconsolidated or poorly consolidated salt.

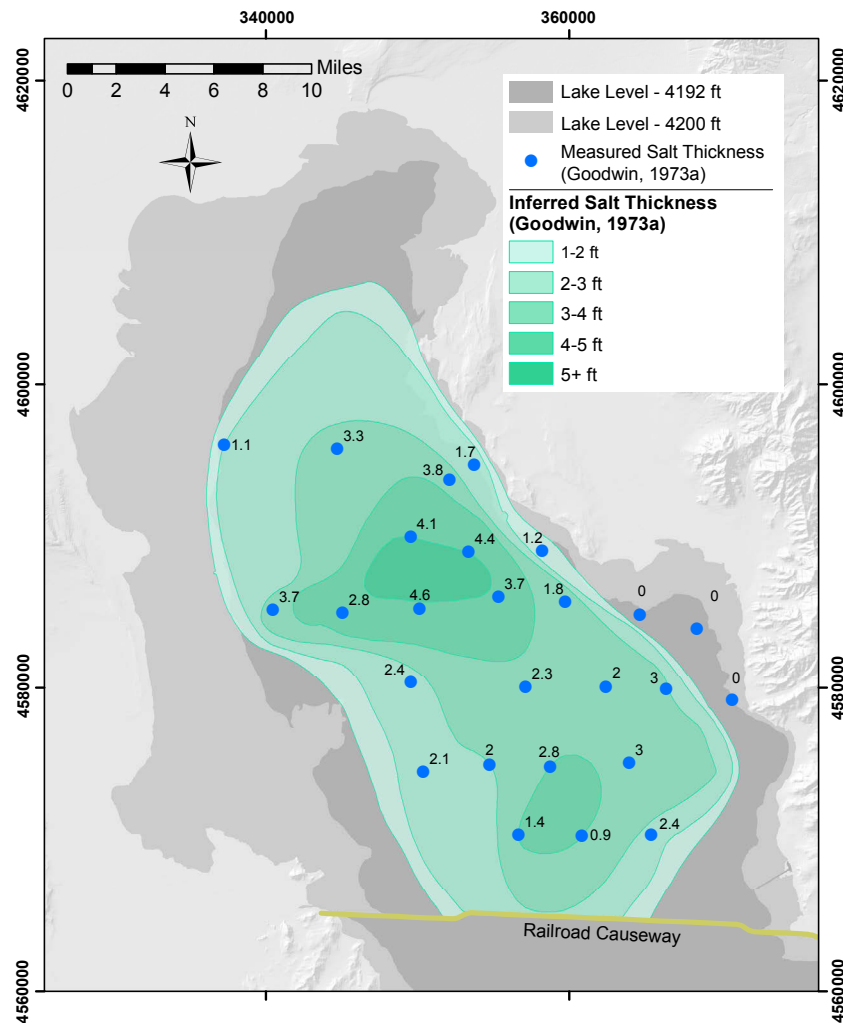


Figure 6. Salt isopach map from Goodwin (1973a). Blue points show salt core locations and labels indicate maximum measured salt thickness in feet as represented in cross sections. Some cores did not intercept the base of the salt and Goodwin (1973a) inferred the salt to be thicker than measured in some areas. Lake levels are based on bathymetry from Baskin and Allen (2005) and Baskin and Turner (2006). Coordinates are UTM Z12 NAD83.

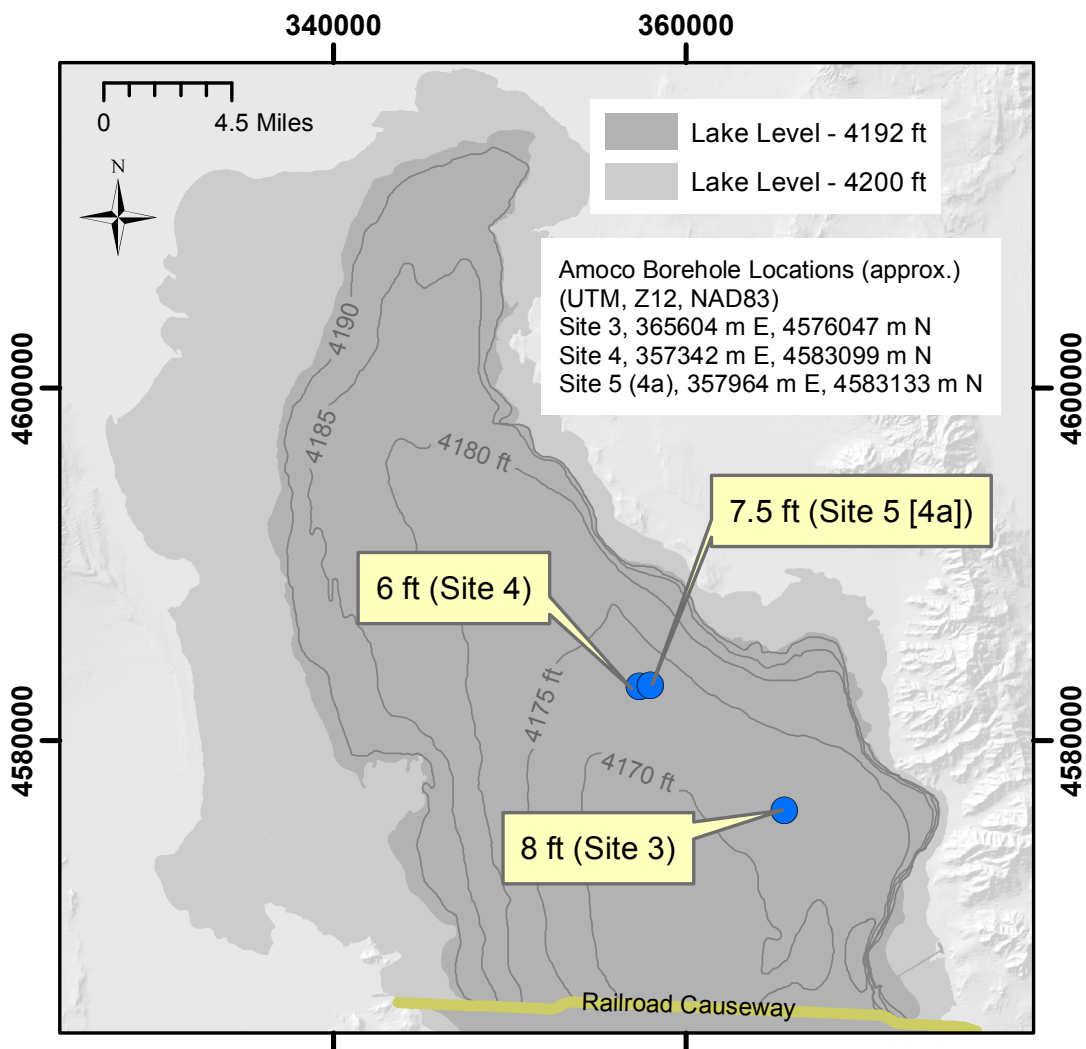


Figure 7. Amoco Production Company borehole locations and salt thickness. Yellow labels indicate salt thickness and site number. Data are from Dames and Moore (undated) and Woodhall (1980). Bathymetry is from Baskin and Turner (2006). Grid coordinates are UTM Z12 NAD83.



Figure 8. In-place, submerged crystalline halite. Note coarse texture and sharp crystal edges. Photograph was taken near transect 9.



Figure 9. Smooth, crystalline salt crust exposed above the lake water level. These smooth, usually pink surfaces represent dissolution and erosion of the salt crust and they form very hard, competent surfaces. Pen is 5.6 inches long.



Figure 10. Channel where runoff has dissolved the salt crust. Older crust is pink to gray and more recent, whiter salt has precipitated and partially refilled the channel with halite. Small white crystals are also forming on the older, pink crust giving it a rough appearance.

Most of our fieldwork occurred during late summer and fall, which are periods of high evaporation so most crystallization is likely occurring at that time. During those times, along some transects, we noted accumulations of fine-grained salt “rafts” in both submerged and exposed areas of the salt crust (figure 11). During warm months, these rafts of halite can be observed forming on the surface of the water. Eventually, when the rafts become large enough, they sink and accumulate on the floor of the lake. This observation along with the previously described character of the submerged salt crust surface suggests two primary modes of salt crust formation: (1) precipitation of in-place, coarse crystals on the lake bed and (2) accumulation of finer-grained salt rafts that formed on the brine surface. These modes of crust formation are consistent with salt deposition and accumulation in similar environments described by Handford (1991). Recent examination of halite sequences in the Dead Sea also prominently shows these two modes of salt formation (Kiro and others, 2016).

Microscopic examination of salt crust thin sections shows halite crystals almost exclusively. The halite crystals are colorless in plane polarized light and show no birefringence in cross-polarized light because of their isometric crystal structure. Many of the crystals exhibit a euhedral, cubic crystal habit indicative of halite (figure 12). The smaller halite crystals tend to be more euhedral, while larger crystals are often subhedral. The subhedral nature of larger crystals is likely a function of crystal growth inhibited by space constraints and subsequent dissolution. Thin zones of pore space are common where larger halite crystals should seemingly be in contact suggesting dissolution along crystal interfaces (figure 13). Random crystal orientation is common, but layered configurations also occur (figure 14). The layers are likely salt rafts that have accumulated on the lake floor and look similar to photomicrographs of preserved rafts in modern halite crust presented in Handford (1991). The thin sections highlight the



Figure 11. Accumulations of salt rafts. Along the east shore of the north arm near transect 4 (top) and along the north shore near transect 3 (bottom). Pen length is 5.6 inches.

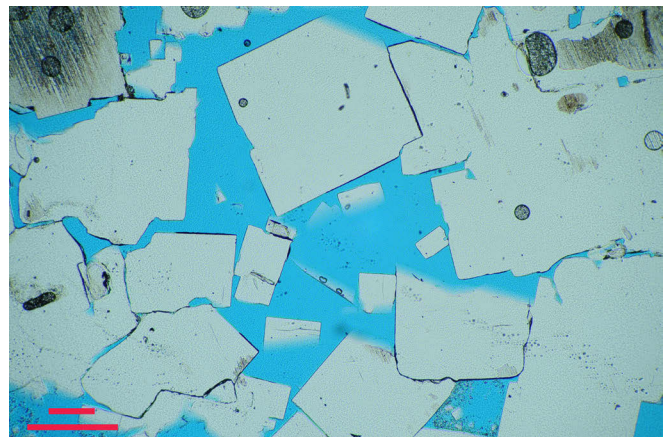


Figure 12. Photomicrograph of halite crystals in the salt crust showing both euhedral and subhedral faces. Euhedral crystal faces show the cubic structure of halite. Blue coloring indicates pore space. Top red line is 0.01 inches and lower red line is 0.5 mm. Thin section is from sample SCI 2 (transect 7).

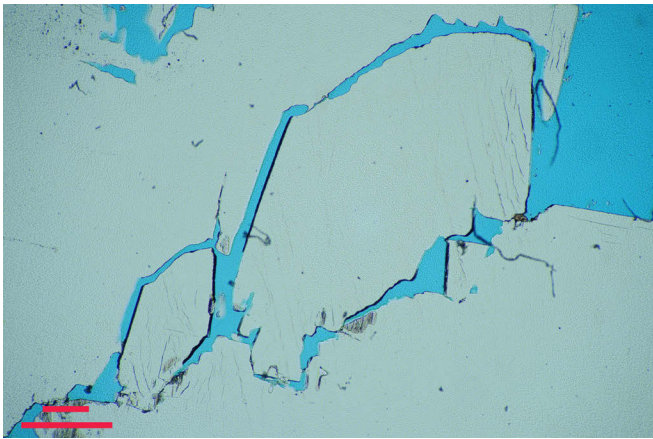


Figure 13. Photomicrograph of large, subhedral halite crystals. Thin pore space (indicated by blue coloring) along crystal boundaries suggests dissolution along interfaces that were previously in contact. Top red line is 0.01 inches and lower red line is 0.5 mm. Thin section is from sample SCI 1 (transect 2).

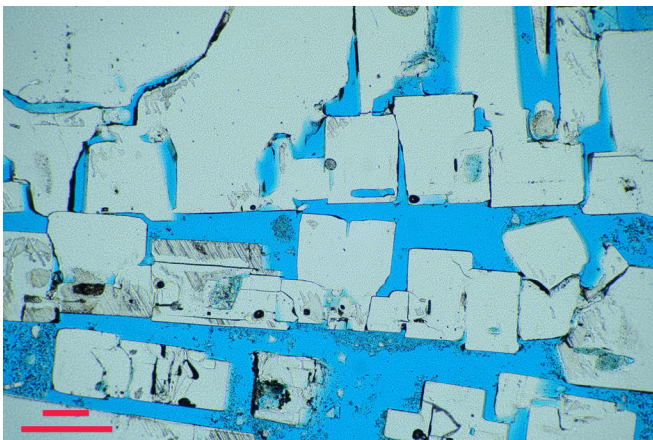


Figure 14. Photomicrograph of layered halite crystals. Horizontal layers likely represent preserved salt rafts that have become assimilated into the salt crust. Blue coloring indicates pore space. Top red line is 0.01 inches and lower red line is 0.5 mm. Thin section is from sample SCI 1 (transect 2).

porosity of the salt crust, but overall show a crystal-supported matrix (figure 15). We observed minor amounts of interstitial gypsum, which were identified by their prismatic shape and lower first-order birefringence (figure 16).

Chemistry and Mineralogy

As previously noted, our analytical results show that the primary constituent of the salt crust is halite (NaCl) (table 1), and these results are consistent with past data (table 2, appendix A). The six chemical analyses (including one duplicate) presented in table 1 are from samples collected at three transect sites (2, 7, and 8; see figure 1 or plate 1 for locations). On average, the weight percent (wt. %) of Na and Cl of those samples is 99.0. Most of the remaining 1% is made up of Mg, K, Ca, and S, which, after Na and Cl, are the primary constituents of the lake brine (Utah Geological Survey, 2016).

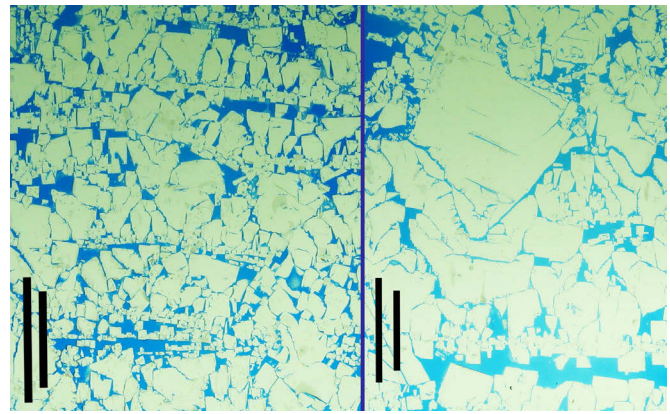


Figure 15. Thin sections showing crystal-supported matrix and pore space. Left image exhibits layering from salt raft accumulations. Blue coloring indicates pore space. For each slide, longer black line is 0.5 inches and shorter black line is 1 cm. Thin sections are from sample SCI 1 (transect 2).

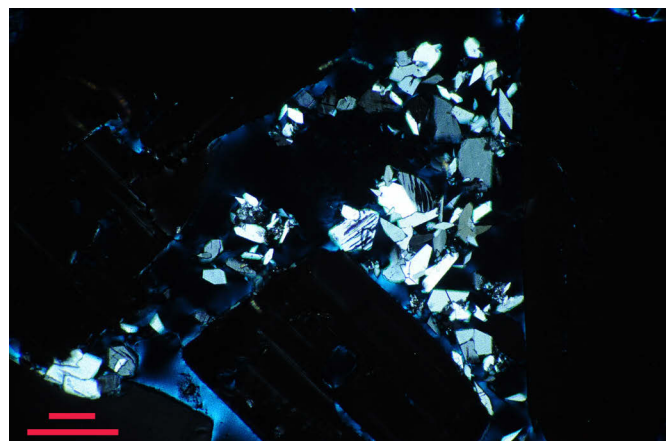
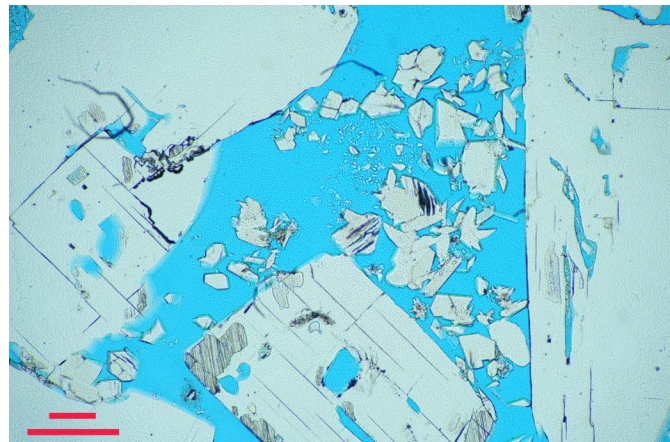


Figure 16. Photomicrographs of halite and gypsum crystals. Both halite and gypsum are clear in plane-polarized light (top), but halite is black in cross-polarized light (bottom) and gypsum shows lower first-order birefringence (white and gray coloring). Some of the birefringent crystals show a prismatic shape, which is another indication of gypsum. Blue coloring indicates pore space (top). Top red line is 0.01 inches and lower red line is 0.5 mm. Thin section is from sample SCI 1 (transect 2).

Table 1. Chemical composition of the salt crust.

Sample Number	Cl wt. %	Na wt. %	Mg wt. %	K wt. %	Ca wt. %	S ppm	Br wt. %	Sr ppm	Li ppm	Insolubles wt. %	Moisture wt. %	Total
SCI 1.2	59.6	39.2	0.03	0.15	0.03	428	0.002	<1	1	0.3	0.2	99.52
SCI 1.4	59.6	39.0	0.03	0.04	0.21	1910	0.002	3	1	0.2	0.3	99.60
SCI 2.2	59.5	39.0	0.04	0.02	0.29	2550	0.002	4	1	0.2	0.4	99.72
SCI 2.4	60.0	39.5	0.04	0.02	0.05	642	0.002	<1	1	0.1	0.3	100.03
SCI 3	60.1	39.5	0.01	<0.01	0.05	416	0.002	<1	<1	0.1	0.1	99.87
SCI 3 R	59.8	39.3	0.01	<0.01	0.05	415	0.002	1	<1	0.1	0.1	99.42

Notes:

1. Samples were collected on the following transects: SCI 1 - transect 2; SCI 2 - transect 7; SCI 3 - transect 8
2. Photos of samples are available in appendix B.
3. Sample SCI 3 R is a rerun of sample SCI 3.

Table 2. Chemical composition of the salt crust as determined by previous studies.

	Handy and Hahl (1966)		
	Hahl and Handy (1969)	Hedberg (1970)	Goodwin (1973a)*
Na	39.9	38.6	36.89 (\pm 3.67)
Mg	0.0	0.0015	0.10 (\pm 0.07)
Cl	59.7	60.4	59.07 (\pm 8.45)
K	0.1	0.004	0.28 (\pm 0.16)
Ca	0.0	0.002	0.26 (\pm 0.38)
SO ₄	0.3	0.0016	1.36 (\pm 2.65)
Br	nr	0.005	nr
Fe	nr	<0.002	nr
Cu	nr	<0.001	nr
H ₂ O (-)	nr	nr	0.40 (\pm 0.49)
Insolubles	nr	0.1	1.5 (\pm 13.66)
Sample Date	1964	1969	1970, 1972

*Average of 46 samples with standard deviation

nr - not reported

Insoluble material in each sample consists of an average of 0.2 wt. %. Detected trace elements in the samples include only Br and Li. Several other elements were analyzed for but fell below detection limits (appendix C). Our results compare well with previous results; however, an average of Goodwin's (1973a) results shows a slightly lower weight percent of Na and Cl (96.0%) and higher amounts of Mg, K, Ca, and S. Our results may be more representative of the crust because Goodwin's (1973a) samples were not drained following collection, so residual lake brine could have precipitated minerals with additional Mg, K, Ca, and S.

We used XRD to evaluate the same set of samples we had chemically analyzed, and XRD confirmed that the crust is almost exclusively halite. All the significant peaks in the XRD spectra were attributable to halite, and, in all five samples, halite had the lowest figure of merit (FOM), which is a measure of how well a diffraction pattern fits a particular mineral. A FOM below 1.0 generally suggests a good fit, and the FOM

for halite ranged from 0.227 to 0.425 and averaged 0.340. Rigaku's PDXL software provides a quantitative analysis of mineral components and indicated halite composition ranging from 97 to 98 wt. %, but with a relatively high error¹. Based on XRD, accessory minerals in the crust may include sylvite, gypsum, carnallite, and montmorillonite. However, because these minerals are in such small amounts (typically a maximum of 1.5 wt. %), they are near minimum XRD detection limits. Of these minerals, sylvite and gypsum had the lowest FOM; the sylvite FOM averaged 0.792 and the gypsum FOM averaged 1.00. Gypsum was detected in two samples, but sylvite was detected in all five samples. We confirmed the presence of gypsum in thin section, but sylvite is nearly identical to halite in thin section and was not specifically identified. Carnallite was not positively identified in thin section, but a few small grains with relatively high birefringence

¹ The error relates to the certainty of weight percent of halite in the sample; it is not necessarily related to FOM. In other words, the FOM strongly suggests there is halite in the sample, but there is uncertainty as to exactly how much.

were noted that could potentially be carnallite. The presence of sylvite or carnallite would almost certainly be a result of evaporation of residual lake brine. The presence of sylvite is questionable as it does not occur along the typical crystallization path of GSL brine (Butts, 1980).

Thickness

Previous thickness measurements of the north arm salt crust range up to 8 ft as reported by Dames and Moore (undated) and Woodhall (1980) (figure 7, plate 1); those and additional measurements from past studies are presented in table 3. Our measurements from nine transects around the north arm (figure 1, plate 1) yielded thickness up to 1.88 ft. Each transect is presented in figures 17 through 25 and the raw data from our measurements are in appendix D. Our data are similar to Goodwin's (1973a) (figure 6) in that they show a general thickening of salt crust from the edge of the salt towards the deeper parts of the north arm in a pattern consistent with what would be expected in a typical sedimentary basin. We measured both exposed and submerged salt crust, and for most transects, salt thickness reached a maximum of about 1 ft or slightly more before our measurements were limited by the brine depth. Based on this observation, we conclude that most of the submerged north arm lake bed had a minimum salt crust thickness of 1 ft during late 2015. However, past data from Goodwin (1973a), Dames and Moore (undated), and Woodhall (1980) show potential for much thicker crust in central parts of the bay.

We projected the location of a 1-ft isopach for the salt crust for late 2015 (figure 26). The location of this contour is approximate, particularly in long stretches between sampling transects, but our consistent observation that about a foot of salt thickness occurred slightly offshore suggests that our estimate is reasonable. We used the 2014 orthophotography and Baskin and Turner's (2006) bathymetry as a guide for inferring the location of the contour between transects. We could not exclusively use Baskin and Turner's (2006) bathymetry because the elevation at which we observed or projected the salt crust to be 1-ft thick is variable and ranged from about

4188 to 4192 ft above sea level. Also, the recent orthophotography reveals rarely exposed lake bed and shows areas that required departure from the bathymetry.

We re-measured salt thickness at selected sites along transect 1 and 2 (figures 1, 17 and 18) in early March and April 2016. Measurements show a decrease in crust thickness at all 11 sites we revisited, and the largest decreases we observed were at submerged locations. We re-measured one submerged site in March and it showed a crust thickness decrease of 0.24 ft since August 2015. About one month later, in April, an additional 0.18 ft had dissolved for a total thickness decrease of 0.42 ft. An additional submerged site we revisited in April showed a decrease in crust thickness of 0.46 ft for the period of August to April. Exposed sites on land also showed a decrease, but the decrease was less significant. The average measured thickness decrease of exposed salt crust from August to April was 0.13 ft. The exposed crust had a dissected appearance in April exhibiting channels of varying size eroded into the crust. At the water's edge the differential in dissolution of the submerged crust and the exposed crust was shown by a receding salt ledge (figure 27). We are uncertain if the dissolution of the submerged crust is a result of freshening of the brine confined to the edge of the lake or from a slight overall freshening of the north arm as the water seasonally rises. Localized freshening at the edge of the lake could be caused by sheet and channel flow into the lake from significant storm events or shallow groundwater flow discharging near the lake margins. Because the increase in water level at the time of our April measurements was minimal (+0.3 ft) from the annual low (4190.6 ft), the dissolution may be more likely related to a localized effect of inflow during rain events. Future crust thickness, precipitation, and salinity data collection could be helpful for interpretation. Hahl and Handy (1969) installed gauges near Rozel Point in July 1964 to monitor salt crust thickness for about two years (table 4). However, interpretation of their data is difficult because the exact locations of the gauges are unknown and periods of submersion and exposure are unclear. Water elevation and salinity data are also unavailable for most of the period of their measurements.

Table 3. Thickness measurements of the salt crust from previous studies.

Reference	Measured Thickness (ft)	Thickness in Original Reported Units	Measurement Year	Notes
Eardley (1970)	0.33	4 in	1961	measurement at shoreline near Rozel Point
Adams (1964)	0.98	30 cm	1963 (?)	unspecified measurement location
Handy and Hahl (1966), Hahl and Handy (1969)	0.67	8 in	1963	measurement at shoreline near Rozel Point
Eardley (1966)	0.33 to 1	4 to 12 in	1964	measurement location(s) not specified
Hedberg (1970), Eardley (1970)	0.33 to 1.15	10 to 35 cm	1969	shoreline thickness measurements
Goodwin (1973a)	0 to 4.6	0 to 4.6 ft	1970, 1972	core holes throughout north arm
Woodhall (1980), Dames and Moore (undated)	6 to 8	2-3 m (6-8 ft)	1974 (August)	core holes from east-central north arm

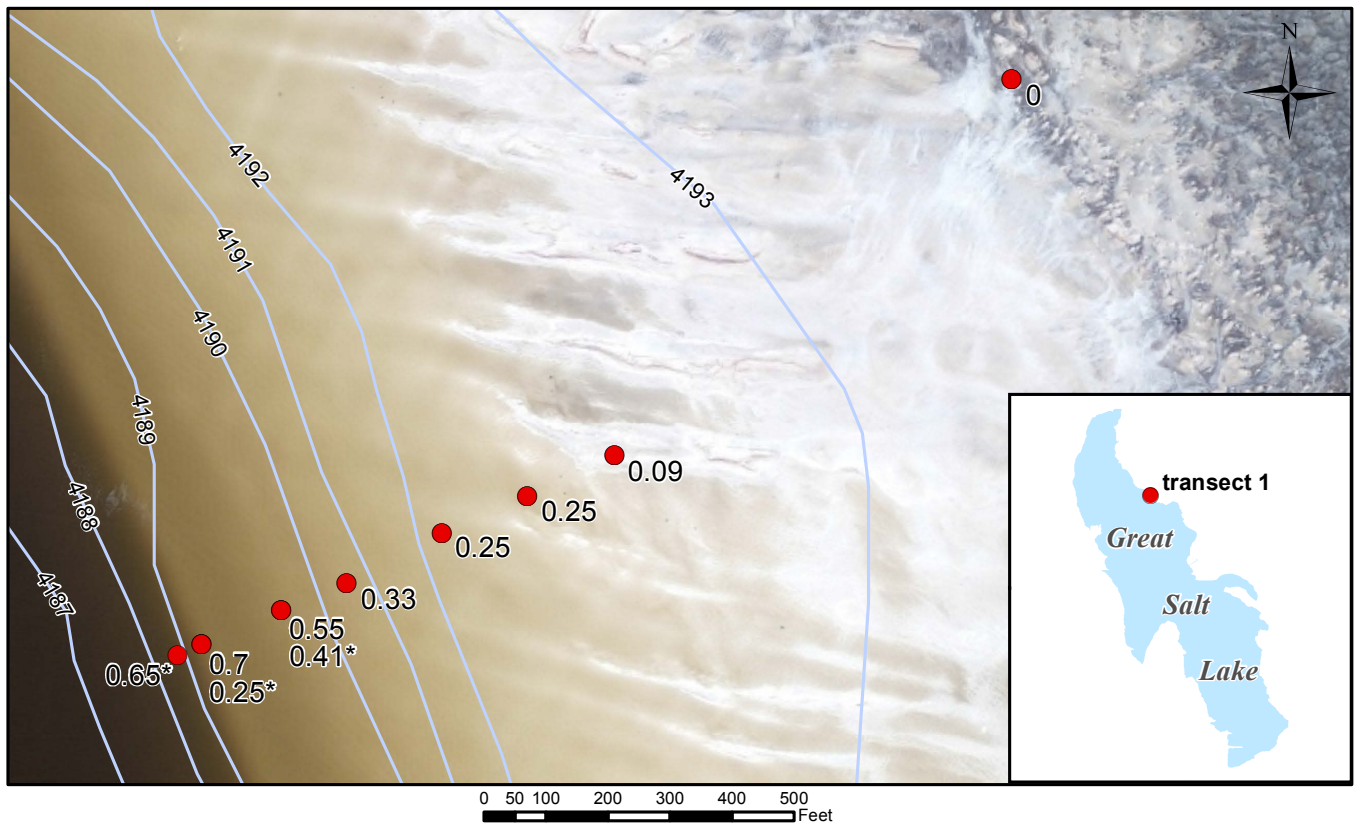


Figure 17. Transect 1 (red points) with salt crust thickness in feet. Thickness measurements collected 8/13/15 and *4/7/16. Light blue lines represent one-foot contour bathymetry from Baskin and Turner (2006). Base imagery is from August 2014 and is provided by Google.

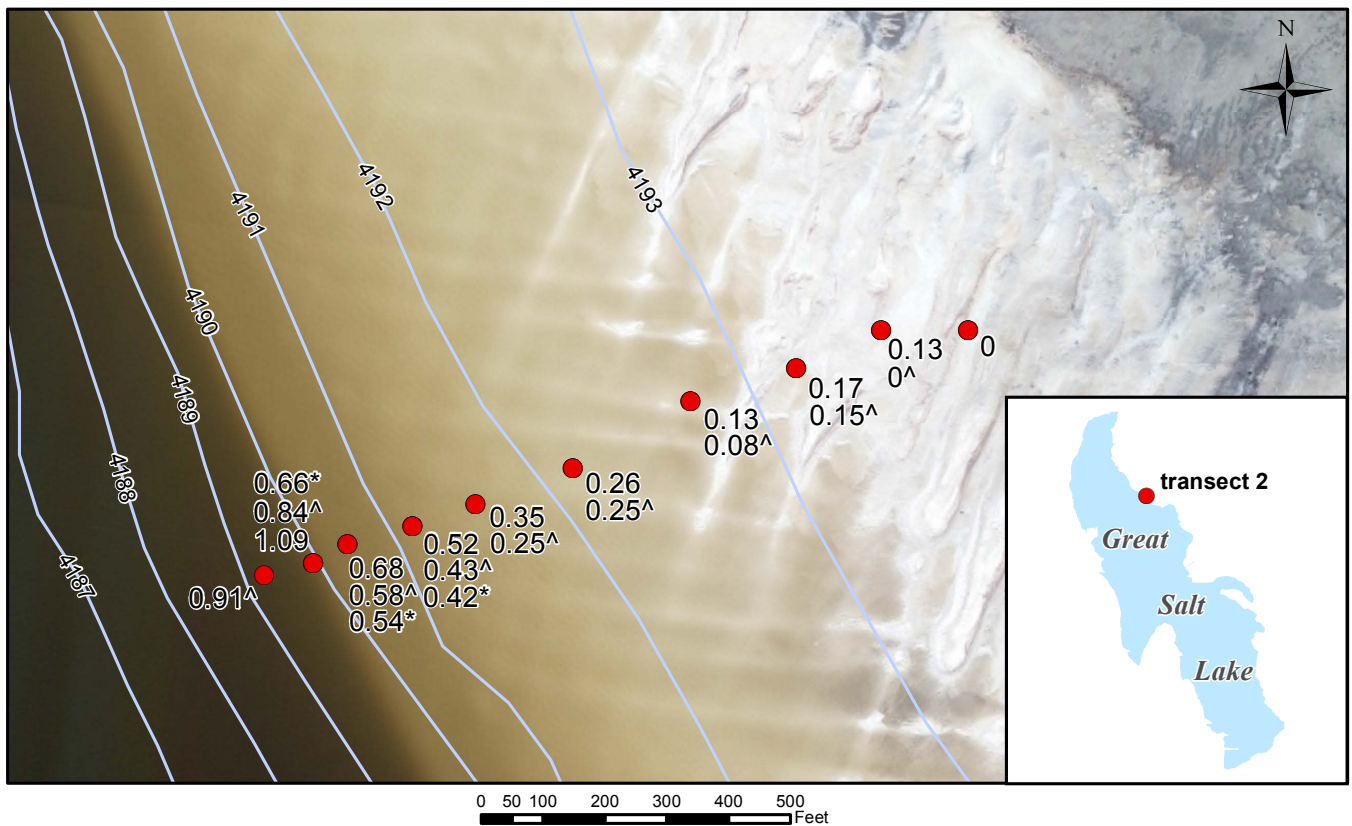


Figure 18. Transect 2 (red points) with salt crust thickness in feet. Thickness measurements collected 8/21/15, ^3/4/16, and *4/7/16. Light blue lines represent one-foot contour bathymetry from Baskin and Turner (2006). Base imagery is from August 2014 and is provided by Google.

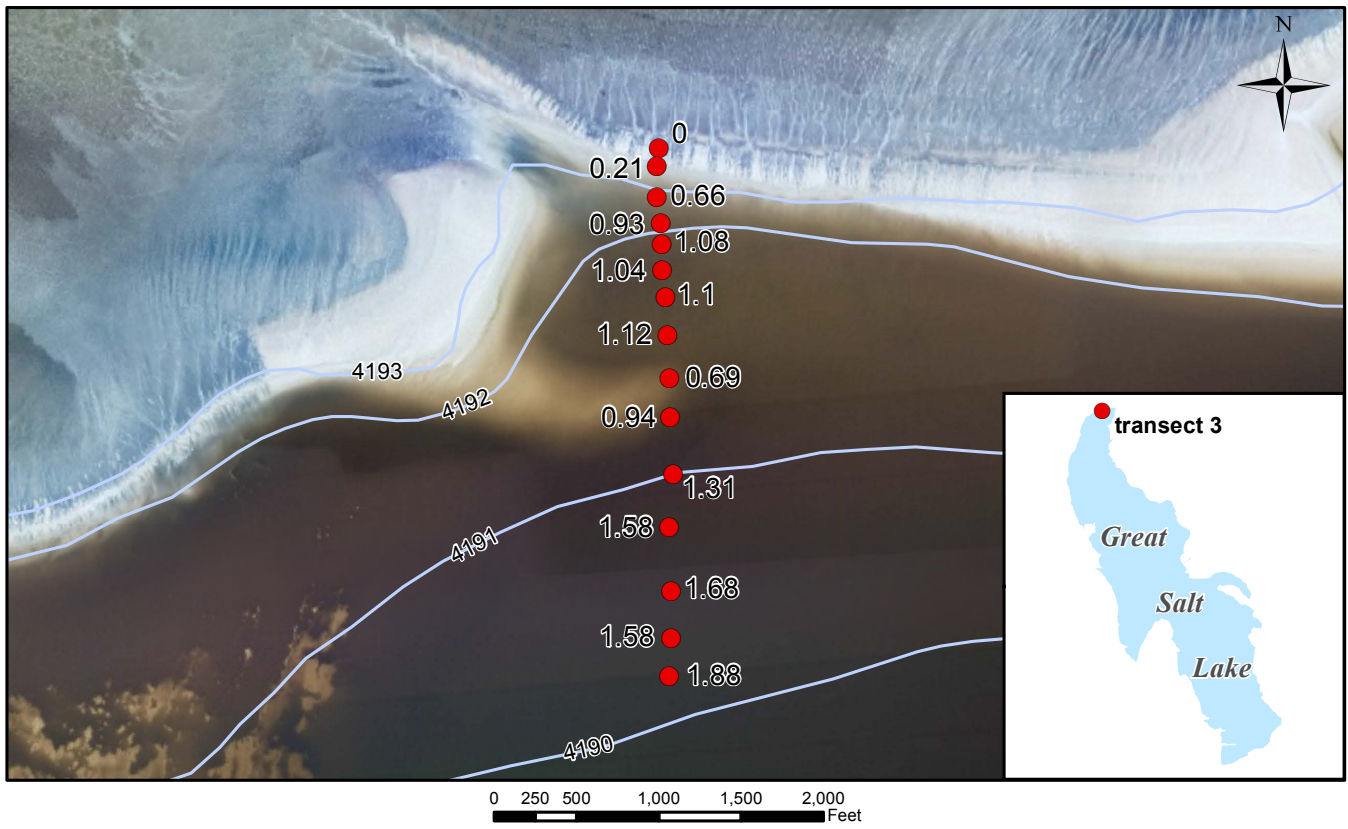


Figure 19. Transect 3 (red points) with salt crust thickness in feet. Thickness measurements collected 8/25/15. Light blue lines represent one-foot contour bathymetry from Baskin and Turner (2006). Base imagery is from August 2014 and is provided by Google.

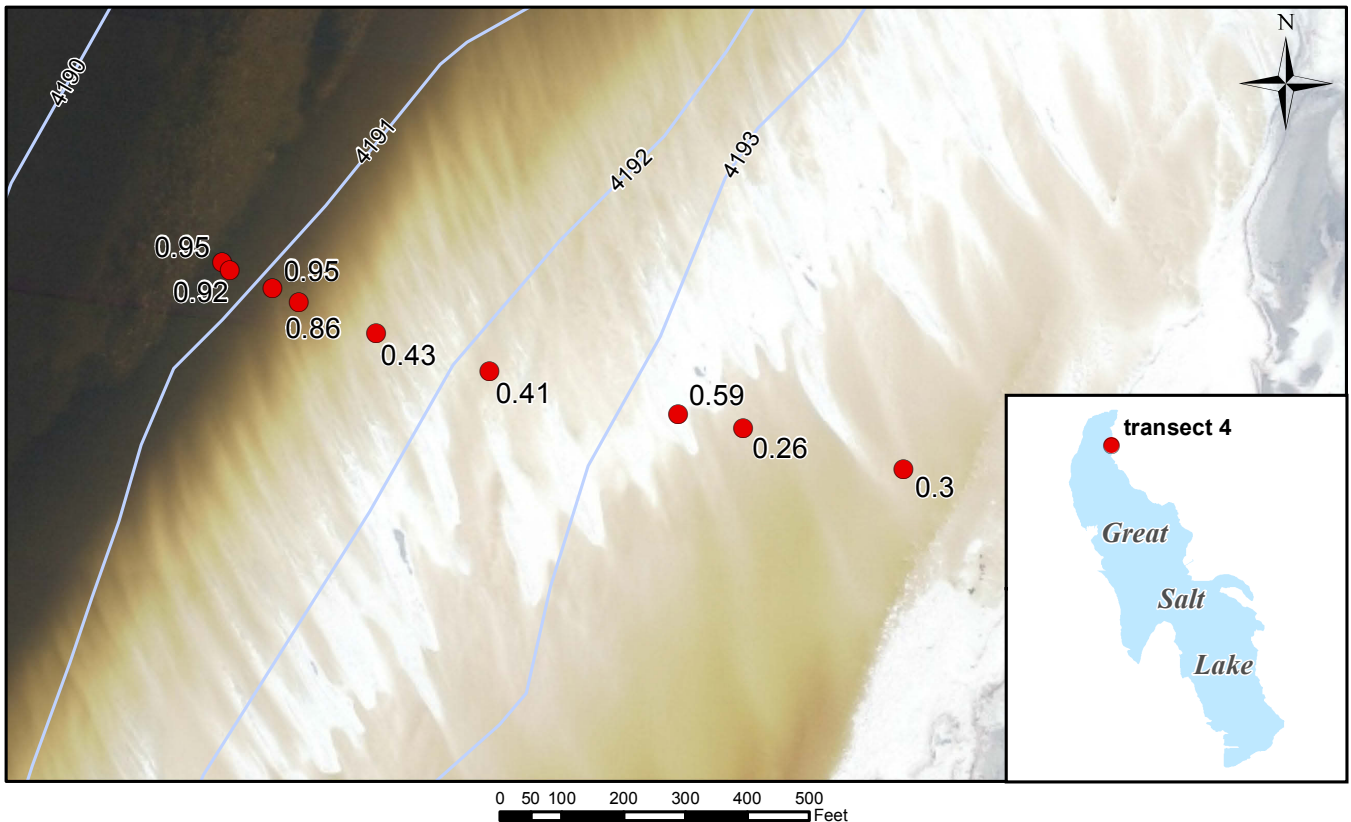


Figure 20. Transect 4 (red points) with salt crust thickness in feet. Thickness measurements collected 8/31/15. Light blue lines represent one-foot contour bathymetry from Baskin and Turner (2006). Base imagery is from August 2014 and is provided by Google.

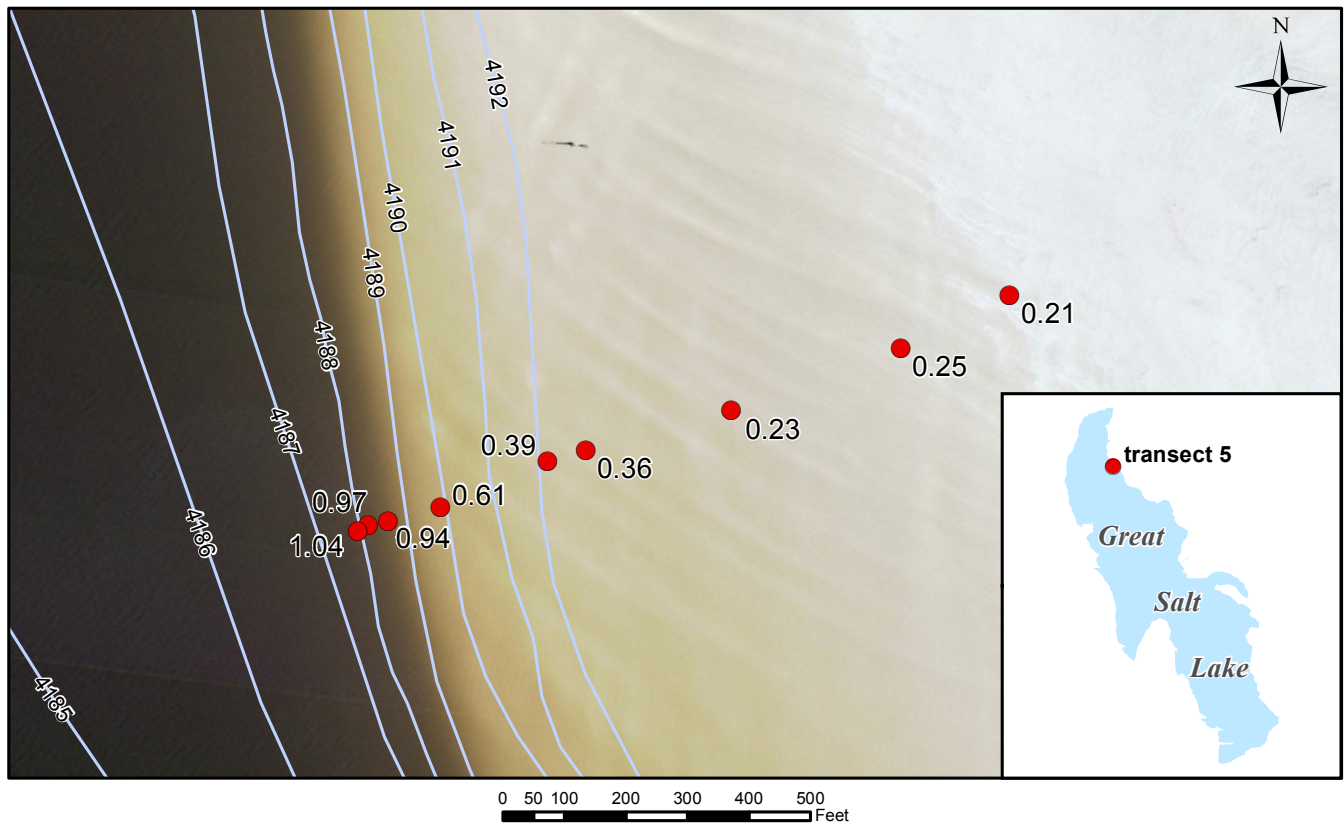


Figure 21. Transect 5 (red points) with salt crust thickness in feet. Thickness measurements collected 8/31/15. Light blue lines represent one-foot contour bathymetry from Baskin and Turner (2006). Base imagery is from August 2014 and is provided by Google.

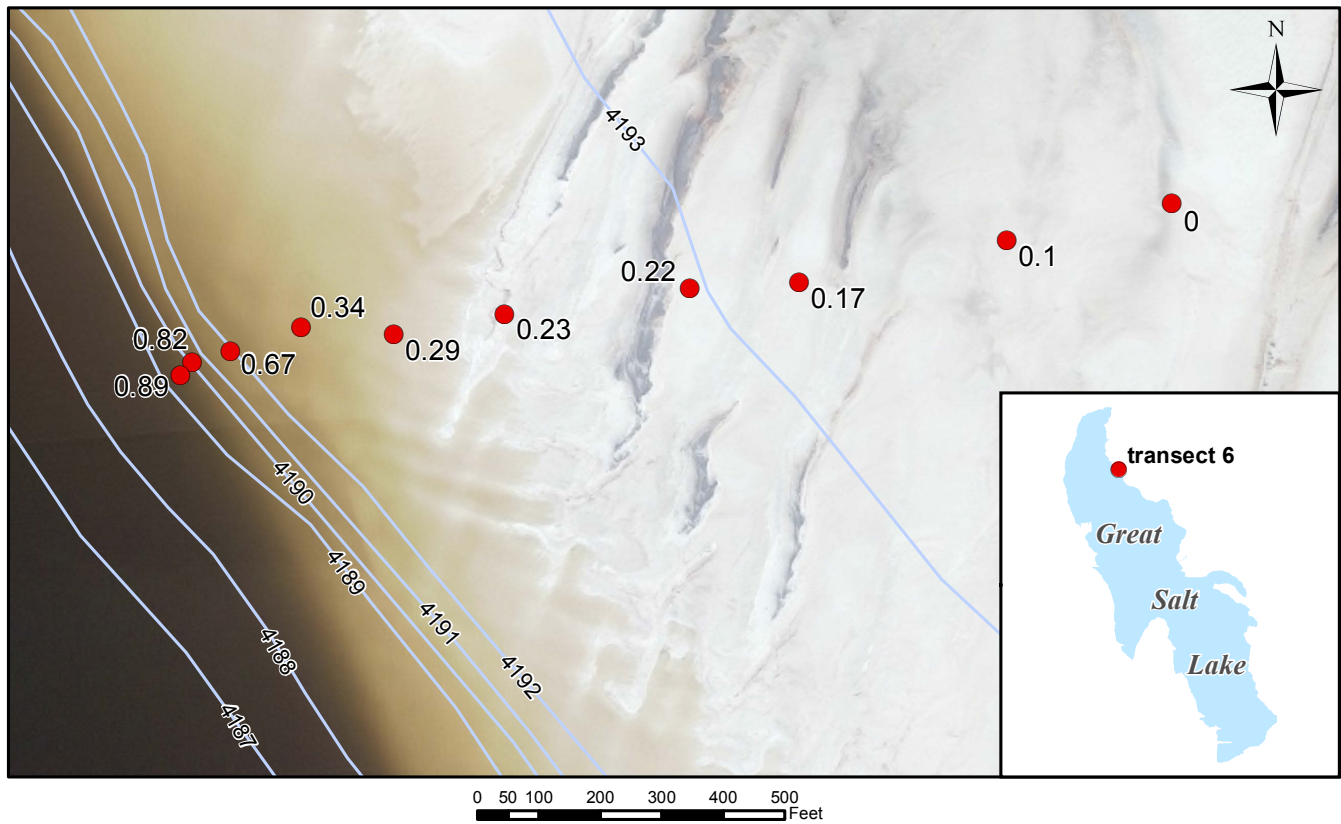


Figure 22. Transect 6 (red points) with salt crust thickness in feet. Thickness measurements collected 9/2/15. Light blue lines represent one-foot contour bathymetry from Baskin and Turner (2006). Base imagery is from August 2014 and is provided by Google.

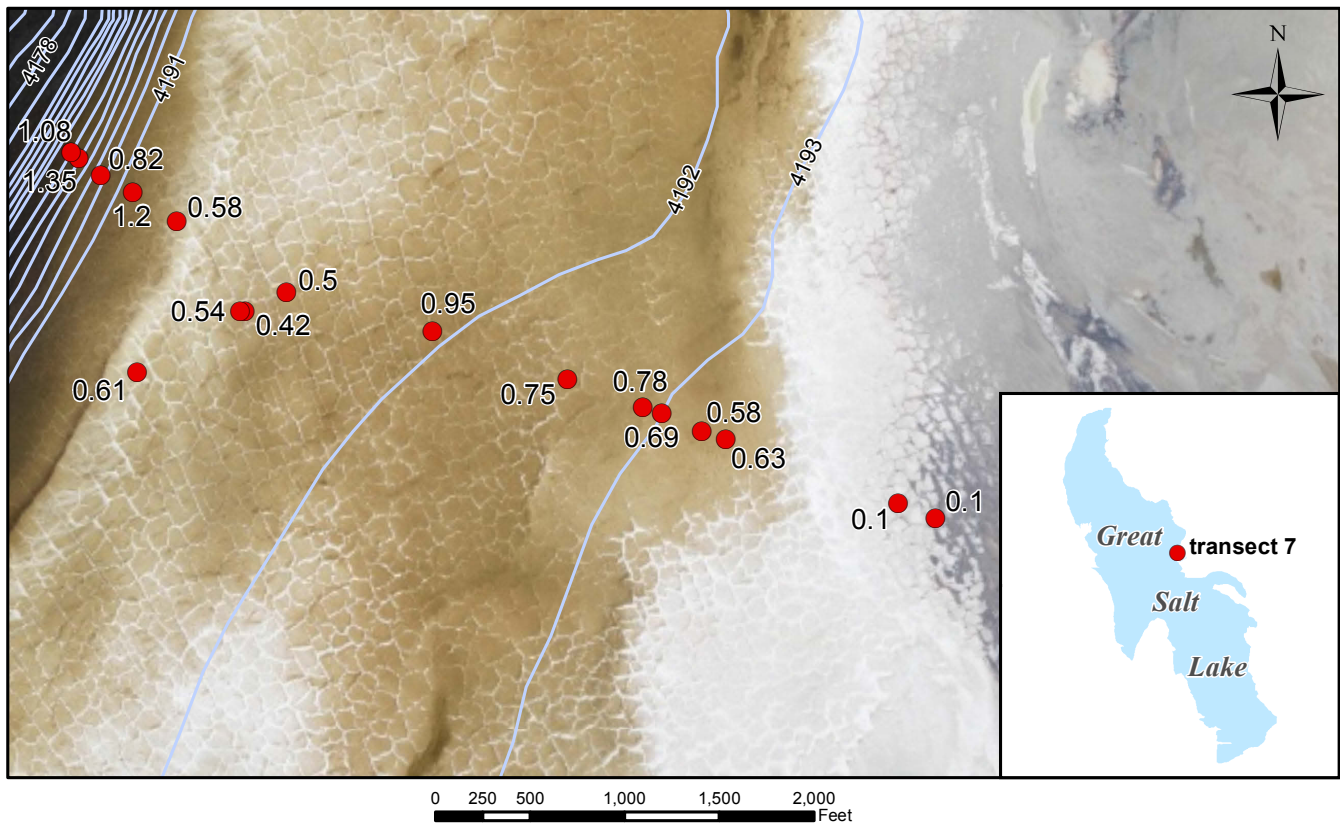


Figure 23. Transect 7 (red points) with salt crust thickness in feet. Thickness measurements collected 9/9/15. Light blue lines represent one-foot contour bathymetry from Baskin and Turner (2006). Base imagery is from August 2014 and is provided by Google.

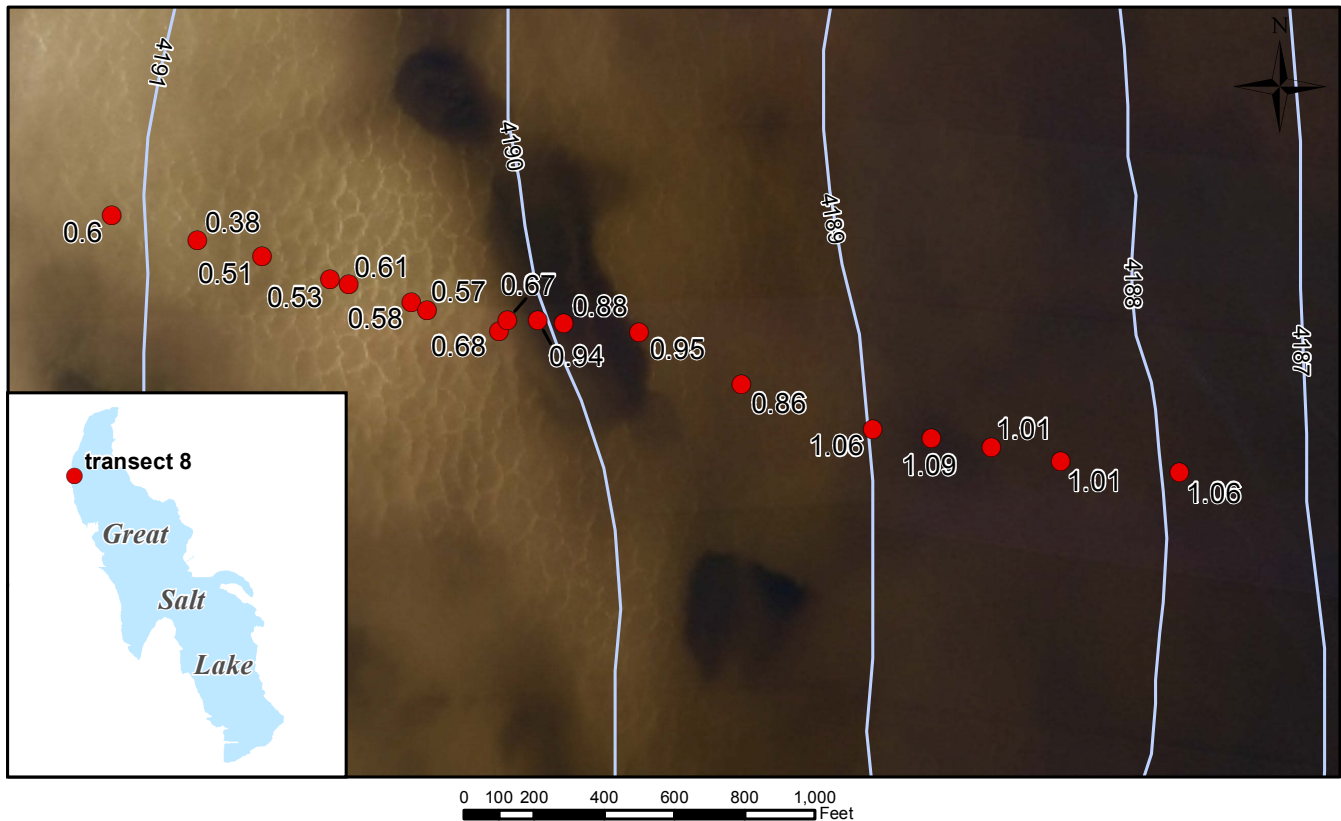


Figure 24. Transect 8 (red points) with salt crust thickness in feet. Thickness measurements collected 9/30/15. Light blue lines represent one-foot contour bathymetry from Baskin and Turner (2006). Base imagery is from August 2014 and is provided by Google.

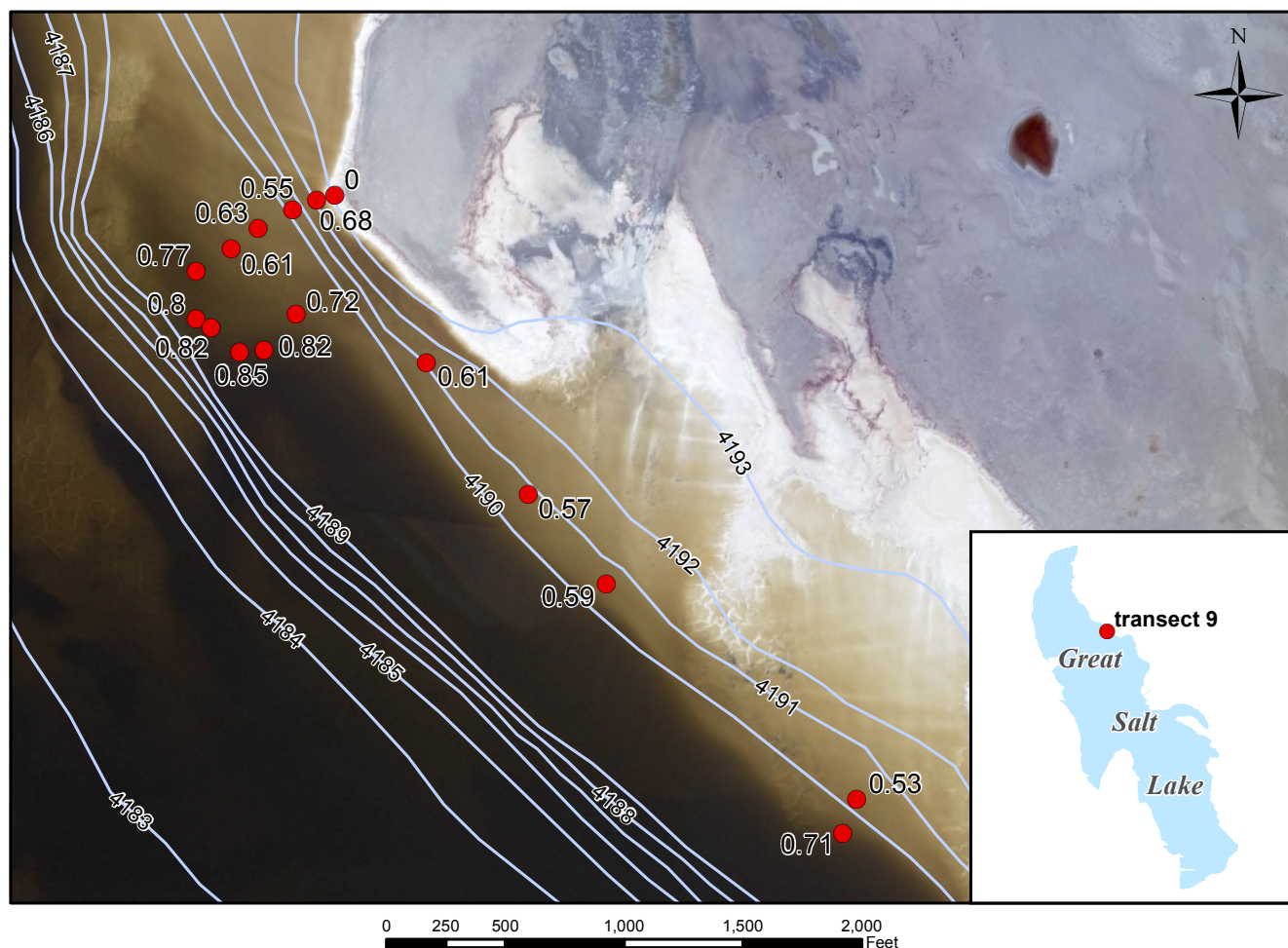


Figure 25. Transect 9 (red points) with salt crust thickness in feet. Thickness measurements collected 11/13/15. Light blue lines represent one-foot contour bathymetry from Baskin and Turner (2006). Base imagery is from August 2014 and is provided by Google.

We were able to re-occupy one of the coring sites (site G-1; appendix A) reported by Goodwin (1973a). We measured a surficial salt crust of 0.56 ft (station 67; appendix D); however, it is difficult to compare our data with Goodwin's (1973a). Goodwin's (1973a) cross sections indicate a surficial salt crust of 0.4 ft at the location, but additional mixed salt and oolitic sand, silt, and mud are present to a depth of about 2.5 ft (appendix A). The part of Goodwin's (1973a) section that represents the recent salt crust is unclear.

North Arm Precipitated Salt Load

Estimates of the precipitated salt load in the north arm of GSL have ranged from 0.6 to 2.2 billion short tons (table 5), but these estimates range in time frame and evaluation method (often unspecified). Eardley (1966) also qualitatively estimated that the salt crust contains about 20% of the total salt load in the GSL system. The estimate based on the most robust dataset is from Goodwin (1973a) in which he calculated a salt load of about 1.1 billion short tons based on his salt isopach map. We attempted to replicate Goodwin's (1973a) calculation using his isopach map, some simple assumptions, GIS methods, and his measured average density of 1.436 g/cm^3 , and our

result was 1.2 billion short tons. Several of the cores from Goodwin's (1973a) study did not completely penetrate the salt crust (appendix A), so the salt may be thicker in some areas than Goodwin (1973a) projected. Amoco's drilling data, which provide salt thicknesses only a few years following the UGS drilling for Goodwin's (1973a) work, support this possibility. Where Amoco encountered 6 to 7.5 ft of salt, Goodwin (1973a) inferred only about 4 ft of salt, and where they encountered 8 ft of salt, Goodwin (1973a) inferred only about 3.5 ft. This suggests that Goodwin (1973a) may have underestimated the precipitated salt load. In an abstract, Goodwin (1973b) estimated a salt crust tonnage of 2.2 billion short tons presumably based on his isopach map, but we are unsure why there is such a large discrepancy between the unpublished report and the published abstract.

As previously noted, several reports have indirectly calculated the precipitated salt load in the entire GSL system based on salinity levels, brine volume, and an estimated total salt load calculated from salinity data collected during periods when the lake level was high enough (and salinity low enough) that no precipitated salt was in the system. The most recent published estimates from Loving and

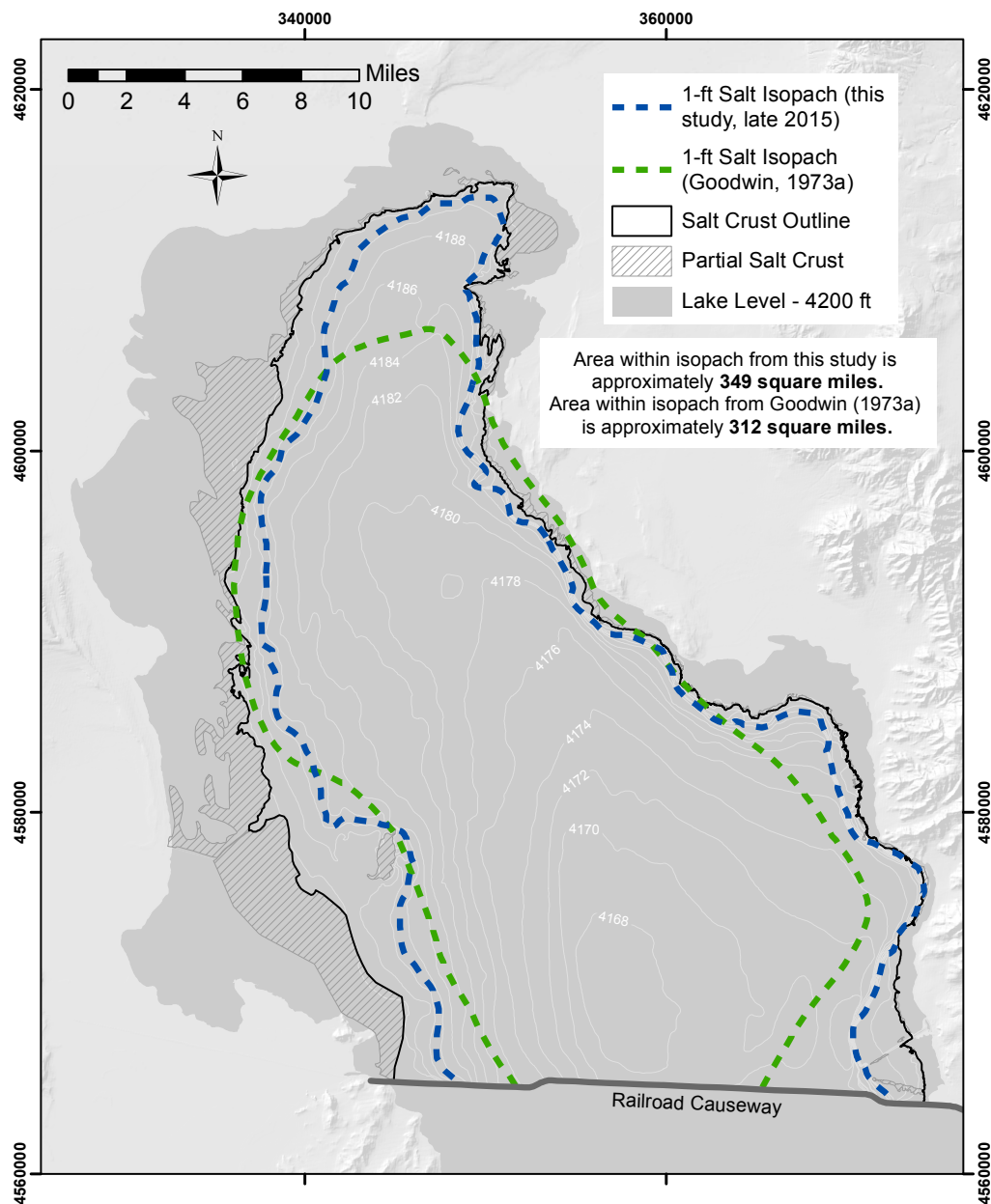


Figure 26. Salt isopach map. Isopach from this study is representative of late 2015. White lines represent two-foot contour bathymetry (feet above mean sea level) from Baskin and Turner (2006). The outermost bathymetric contour is 4194 ft. Grid coordinates are UTM Z12 NAD83.

others (2000) and Mohammed and Tarboton (2012) suggest that the maximum amount of precipitated salt at any given time since 1965 is slightly less than 1 billion short tons (figure 28). These estimates of precipitated salt presumably include some salt in evaporation ponds of mineral extraction operations so not all of the calculated tonnage necessarily reflects precipitation in the north arm. Both Loving and others' (2000) and Mohammed and Tarboton's (2012) modeling begins around 1965 and indicates precipitated salt in the GSL system for their entire period of modeling with the exception of about 1986 to 1993 when lake levels were exceptionally high. Goodwin's (1973a) results, particularly in combination with the Amoco drilling data, suggest that these indirect calculations of precipitated salt load in the north arm might be low.

Using our 1-ft isopach (figure 26), which encloses an area of about 349 square miles, and assuming a constant thickness of 1 ft, we estimate a minimum precipitated salt load of 436 million short tons within the isopach for late 2015. Our estimate assumes a salt crust density of 1.436 g/cm³ based on Goodwin (1973a). In addition, we estimate about 20 million short tons of salt in the remaining 65 square miles of thin salt crust outside of the 1-ft isopach. We used an average thickness of 0.25 ft for this area to be conservative and to take into account some dissolution of the outer edge of our mapped crust from 2014 to 2015. These tonnages give a total minimum precipitated salt load of 456 million short tons for late 2015. We did not include any tonnage for areas that we mapped as having only partial coverage of salt crust.



Figure 27. The water's edge near Spiral Jetty (transect 2). During late 2015 the shore was generally a smooth slope into the water (top). Rough-looking white areas in the left half of photo are foam (top). During April 2016 the water's edge was a ledge of receding salt crust due to significant dissolution of the submerged salt crust (bottom). A thin veneer of oolitic sand, silt, and mud covered the submerged salt crust, suggestive of significant fresh inflow from rain events.

Table 4. Salt gauge data from Hahl and Handy (1969).

Time Period	Accumulation (+) or loss (-) in inches		
	Gage 1	Gage 2	Gage 3
July 17, 1964 - Oct. 15, 1964	+3.5 (s?)	+0.5 (s & ex?)	-0.8 (ex)
Oct. 15, 1964 - July 1965	-4.5 (s?)	+0.5 (s & ex?)	-0.2 (ex)
July 1965 - Oct. 6, 1965	+1.3 (s?)	+0.8 (s & ex?)	-1.0 (ex)
Oct. 6, 1965 - May 25, 1966	no data	-7.3 (s?)	-2.2 (ex)

Note: For gauge measurements (s) indicates submerged, (ex) indicates exposed; inferred from Hahl and Handy's (1969) notes.

Table 5. Tonnage estimates of precipitated salt in the north arm of Great Salt Lake from previous studies.

Reference	Estimated Tonnage (million short tons)	Tonnage in Original Reported Units	Estimate Timeframe	Note
Adams (1964)	1100	1 billion metric tons	1963 (?)	
Cohenour (1966)	730	730 million short (?) tons	1963	reportedly based on Adams (1964)
Hedberg (1970)	600	600 million short tons	1969	
Waddell and Bolke (1973), Waddell and Fields (1977)	1140	1.14 billion short tons	1970	based on Goodwin's work
Waddell and Bolke (1973), Waddell and Fields (1977)	1330	1.33 billion short tons	1972	based on Goodwin's work
Goodwin (1973a)	1100	1 billion metric tons	1970 or 1972 (?)	
Goodwin (1973b)	2200	2 billion metric tons	1970 or 1972 (?)	
Waddell and Fields (1977)	1000	1 billion short tons	1974	

The actual precipitated salt load is almost certainly much higher based on our measurements from transect 3 (1.88 ft) and previous data from more central parts of the north arm that show potential for thicker salt. Our 1-ft isopach is comparable (yet 12% larger in area) to Goodwin's (1973a) 1-ft isopach (figure 26, plate 1). If the current halite depositional pattern is similar to what Goodwin's (1973a) data suggest for the early 1970s, then the salt load during late 2015 was likely over 1 billion short tons. Also, although modeling suggests the salt crust was completely dissolved in the late 1980s and early 1990s, Mohammed and Tarboton (2012) estimated high amounts of precipitated salt (nearly 1 billion short tons) toward the end of their modeled time frame in 2006 that are comparable to their projected precipitated levels in the early 1970s when thick salt was measured (figure 28). Given declining lake levels since 2006, the precipitated salt load has likely increased rather than decreased.

CONSIDERATIONS FOR FUTURE STUDY

Future monitoring and study of the salt crust will be helpful to understand and quantify the salt crust's effects on the lake system, and it will also help develop an understanding

of how the salt crust responds to short-term seasonal changes and longer term changes such as causeway modifications and changing lake levels. Some observations made during this study should be considered in future monitoring. Using our method of thickness measurement, transects used for monitoring should be in areas where microbialite mounds are not prevalent. Our experience suggests that microbialite mounds increase measurement error by making the base of the salt more difficult to distinguish from the underlying sediment. Microbialite mounds also introduce significant thickness variability over short distances.

To correctly interpret and understand changes over time, reporting should include information about whether each measurement site is submerged or exposed because our results suggest this can make a significant impact on crust thickness. Additionally, we are uncertain if the dissolution we observed from August 2015 to April 2016 reflects marginal freshening of the brine from storm inflow or a slight overall freshening of the north arm brine from seasonal inflow from the south arm. Measuring salt crust thickness farther from the shore would be helpful in making this determination. Additional salinity monitoring in multiple locations of the north arm could also be helpful in determining whether

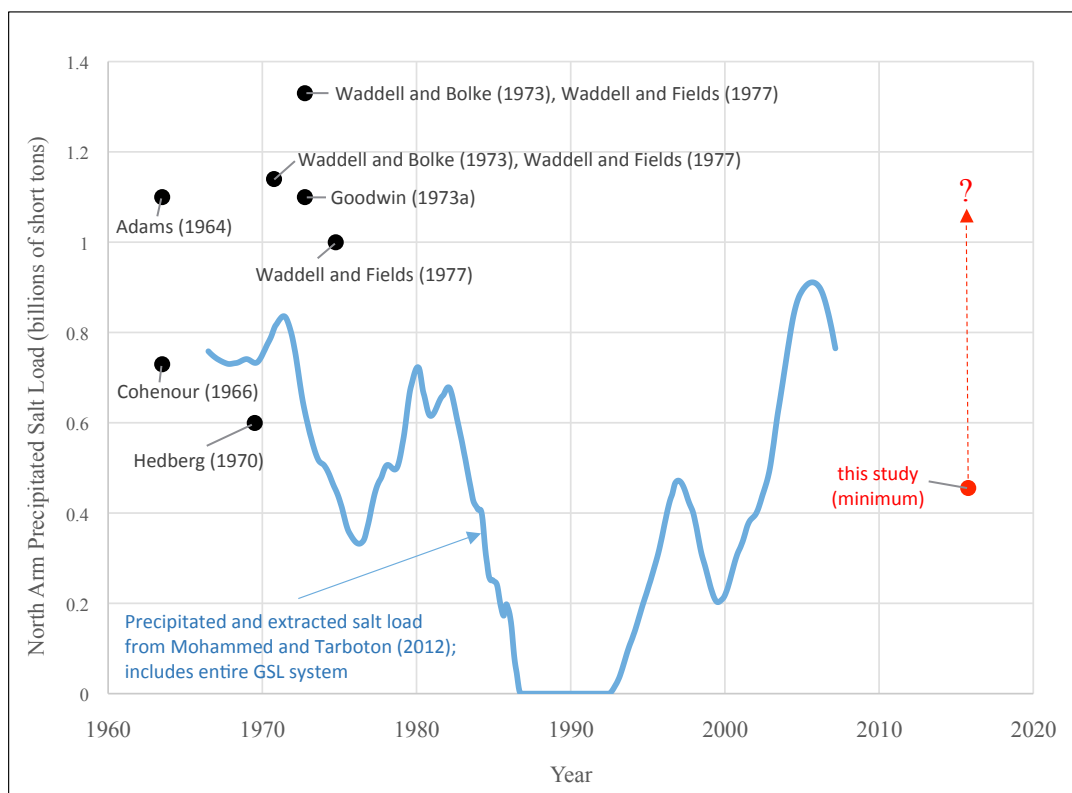


Figure 28. Estimates of the precipitated salt load in the north arm of Great Salt Lake from 1963 through 2015 (excludes Goodwin [1973b]).

periodic freshening of the brine is primarily marginal or throughout the north arm. Ultimately, developing a method to measure salt crust thickness farther from the shore is critical in producing a more accurate precipitated load estimate through direct measurement. The possible discrepancy between precipitated salt load estimates from direct and indirect methods also illustrates the need for better methods to measure the salt crust in central parts of the bay.

CONCLUSIONS

Our mapping indicates that during the latter part of 2014, the north arm salt crust covered an area of roughly 414 square miles and partially covered an additional area of about 52 square miles. Our examination and analysis of the crust shows that it is composed almost exclusively of halite (about 99%) with few accessory minerals. Nearshore thickness measurements from around the perimeter of the north arm yielded crust thickness up to 1.88 ft. During late 2015 the crust was about 1 ft thick a short distance into the lake from the water's edge, and our estimate of a 1-ft salt isopach around the north arm encloses an area of about 349 square miles. This area indicates a precipitated salt load of 436 million short tons, and we conservatively estimate an additional 20 million short tons for the 65 square miles of salt crust outside of our 1-ft isopach. Thus a minimum salt load estimate for late 2015 is 456 million short tons. Given our maximum measured thickness (1.88 ft) and data from previous investigations showing

potential for several feet of salt in central parts of the north arm, the actual precipitated salt load is almost certainly much higher than our minimum estimate. Current low lake levels and a comparison of the pattern of our data to Goodwin's (1973a) data suggest that the actual precipitated salt load is likely in excess of 1 billion tons. The likelihood of significant precipitated salt tonnage in the north arm and a possible underestimation of tonnage by indirect methods show the need for additional research.

ACKNOWLEDGMENTS

We thank the Division of Forestry, Fire, and State Lands for funding this project. We are grateful to Lynn Defreitas, executive director of Friends of Great Salt Lake, for supporting the project in a variety of ways. John Hollenhorst, Ben Tidwell, and Marc Weaver of KSL Channel 5 news arranged and provided helicopter transportation to the west side of the north arm. Thanks to Wes Quinton and Farmland Reserve, Inc., for allowing us to access the northeast portion of Gunnison Bay. Thanks to Ibrahim Mohammed and David Tarboton for providing us with tabular data of their salt load calculations. Wally Gwynn, Ken Krahulec, Craig Morgan, Stephanie Carney, Kimm Harty, and Rick Allis provided helpful reviews of the document.

REFERENCES

- Adams, T.C., 1964, Salt migration to the northwest body of Great Salt Lake, Utah: *Science*, v. 143, no. 3610, p. 1027–1029.
- Baskin, R.L., and Allen, D.V., 2005, Bathymetric map of the south part of Great Salt Lake, Utah, 2005: U.S. Geological Survey Scientific Investigations Map 2894, 1 plate.
- Baskin, R.L., and Turner, J., 2006, Bathymetric map of the north part of Great Salt Lake, Utah, 2006: U.S. Geological Survey Scientific Investigations Map 2954, 1 plate.
- Butts, D.S., 1980, Chemistry of Great Salt Lake brines in solar ponds, *in* Gwynn, J.W., editor, *Great Salt Lake—a scientific, historical and economic overview*: Utah Geological and Mineral Survey Bulletin 116, p. 169–173.
- Cohenour, R.E., 1966, Industrial development and potential of Great Salt Lake with notes on engineering geology and operational problems, *in* Stokes, W.L., editor, *Guidebook to the geology of Utah*: Utah Geological Society Publication 20, p. 153–163.
- Dames and Moore, undated, Drill logs from the 1974–1975 Great Salt Lake soil boring program: unpublished report for Amoco Production Company, unpaginated.
- Eardley, A.J., 1966, Sediments of Great Salt Lake, *in* Stokes, W.L., editor, *Guidebook to the geology of Utah*: Utah Geological Society Publication 20, p. 105–120.
- Eardley, A.J., 1970, The Great Salt Lake—Its history, water levels, salt variations, *in* Joint report on salt distribution problems in Great Salt Lake: unpublished report prepared for Hardy, Morton, and Solar Salt Companies, p. 1–8.
- Goodwin, J.H., 1973a, Composition and lithology of the salt crust, North Arm, Great Salt Lake, Utah: unpublished report prepared by the Utah Geological and Mineral Survey, 12 p.
- Goodwin, J.H., 1973b, Salt deposition in north arm, Great Salt Lake, Utah [abs.]: *American Association of Petroleum Geologists Bulletin*, v. 57, p. 957.
- Hahl, D.C., and Handy, A.H., 1969, Great Salt Lake, Utah—chemical and physical variations of the brine, 1963–1966: *Utah Geological and Mineralogical Survey Water-Resources Bulletin* 12, 33 p.
- Handford, C.R., 1991, Marginal marine halite—sabkhas and salinas, *in* Melvin, J.L., editor, *Developments in sedimentology 50—Evaporites, petroleum and mineral resources*: New York, Elsevier, p. 1–66.
- Handy, A.H., and Hahl, D.C., 1966, Great Salt Lake—Chemistry of the water, *in* Stokes, W.L., editor, *Guidebook to the geology of Utah*: Utah Geological Society Publication 20, p. 135–151.
- Hedberg, L., 1970, Salt forms crust in Great Salt Lake: *Utah Geological and Mineralogical Survey Quarterly Review*, v. 4, no. 1, p. 5.
- Kiro, Y., Goldstein, S.L., Lazar, B., and Stein, M., 2016, Environmental implications of salt facies in the Dead Sea: *Geological Society of America Bulletin*, v. 128, i. 5–6, p. 824–841 (doi: 10.1130/B31357.1).
- Klein, C., and Hurlbut, C.S., Jr., 1993, *Manual of mineralogy—21st edition*: New York, John Wiley and Sons, Inc., 681 p.
- Loving, B.L., Waddell, K.M., and Miller, C.W., 2000, Water and salt balance of Great Salt Lake, Utah, and simulation of water and salt movement through the causeway: U.S. Geological Survey Water-Resources Investigations Report 00-4221, variously paginated.
- Madison, R.J., 1970, Effects of a causeway on the chemistry of the brine in Great Salt Lake, Utah: *Utah Geological and Mineralogical Survey Water-Resources Bulletin* 14, 52 p.
- Mohammed, I.N., and Tarboton, D.G., 2012, An examination of the sensitivity of the Great Salt Lake to changes in inputs: *Water Resources Research*, v. 48, no. W11511, 17 p.
- Utah Geological Survey, 2016, Great Salt Lake brine chemistry database: Online, http://geology.utah.gov/docs/xls/GSL_brine_chem_db.xlsx, accessed April 2016.
- Waddell, K.M., and Bolke, E.L., 1973, The effects of restricted circulation on the salt balance of Great Salt Lake, Utah: *Utah Geological and Mineral Survey Water Resources Bulletin* 18, 54 p.
- Waddell, K.M., and Fields, F.K., 1977, Model for evaluating the effects of dikes on the water and salt balance of Great Salt Lake, Utah: *Utah Geological and Mineralogical Survey Water Resources Bulletin* 21, 54 p.
- Whelan, J.A., 1973, Great Salt Lake, Utah—chemical and physical variations of the brine, 1966–1972: *Utah Geological and Mineralogical Survey Water Resources Bulletin* 17, 24 p.
- Whelan, J.A., and Petersen, C.A., 1975, Great Salt Lake, Utah—chemical and physical variations of the brine, water-year 1973: *Utah Geological and Mineralogical Survey Water Resources Bulletin* 20, 29 p.
- Wold, S.R., Thomas, B.E., and Waddell, K.M., 1997, Water and salt balance of Great Salt Lake, Utah, and simulation of water and salt movement through the causeway: U.S. Geological Survey Water-Supply Paper 2450, 64 p.
- Woodhall, R.J., 1980, Engineering problems of Great Salt Lake, Utah, marine oil drilling operation, *in* Gwynn, J.W., editor, *Great Salt Lake—a scientific, historical and economic overview*: Utah Geological and Mineral Survey Bulletin 116, p. 377–392.

APPENDICES

Appendix A

Goodwin (1973a) Report Summary

Goodwin (1973a) provided information on a core drilling program conducted in the north arm of GSL during 1970 and 1972 by the UGMS for the purpose of examining the salt crust. Our Goodwin (1973a) reference consists of unpublished data and reports from the files of the Utah Geological Survey (UGS). The various components include two versions of one report titled *Composition and Lithology of the Salt Crust, North Arm, Great Salt Lake, Utah*, and multiple maps housed within the Energy and Minerals Program of the UGS. A few of the maps include file numbers: 1360-F, UGMS File No. 1567 E, and UGMS File No. 1578 E. A final component is a set of cross sections available in the UGS library titled "Diagrammatic core logs sample line A-G, north arm of Great Salt Lake, Utah." The latest date on several of these components is 1973, so we have assigned that date to the collection of materials. We have combined these materials because the various components provide information relevant to the other components and are generally incomplete as stand-alone documents. We presented some of Goodwin's data in the body of our report, but most of Goodwin's report is presented below and is from what we believe to be the most recent version of the text. We have included minor commentary indicated by [brackets] and some minor editorial corrections were made to the text.

Tables A1 and A2 were compiled for this report summary, tables A3 through A7 were reproduced as is, and figure A1 is based on Goodwin's maps and has been updated for this summary. In the UGS files, two versions of Goodwin's isopach map are available. The versions have the same date with only slight variation in locations of isopach lines, and we have chosen to present the isopachs from the map that contains a UGMS file number (1578 E). However, the alternate isopach map includes some additional information that is compiled and presented in table A1 and figure A1.

Text from Goodwin (1973a):

INTRODUCTION

The Great Salt Lake, located in northwestern Utah, has been the object of concentrated study by the UGMS since the early 1960s. Changes in the water level of the lake because of varying inflow, variations in the total dissolved load, and the effects of construction of a semi-permeable, rock-fill causeway across the lake have strongly affected industries dependent upon the lake in recent years. Beginning in 1963, salt precipitation began in the isolated part of the Great Salt Lake north of the railroad causeway. In 1970 and again in 1972, the UGMS took cores of the salt crust in this northern arm of the lake for the purpose of determining the distribution and thickness of the salt crust and its mineralogical and chemical composition.

Sampling Methods

Cores were obtained by driving 1.5 inch (3.8 cm) diameter galvanized steel pipe into the salt with a fence post hammer. The UGMS's 42 ft (12.8 m) research vessel G.K. Gilbert was used as the working platform. Core tubes were driven either until further penetration became impossible, or until a sudden increase in the rate of penetration suggested that the salt crust had been completely cored and the tube had entered the soft muds beneath the salt crust. Core tubes were extracted from the bottom with the power davit on the Gilbert.

The ends of the tubes were plugged by driving a plastic plug into the inside of the tube and then wrapping the tube with a thick coating of masking tape. Cores taken in 1970 were stored unopened for up to 18 months before analysis was begun. Cores taken in 1972 were sealed in the same way as those taken in 1970, but were opened for sampling no more than 6 months after being taken from the lake. Core tubes were split lengthwise at the University of Utah machine shop. The initial cut with the milling machine was made with standard oil lubricant for the cutting head, but the cut was not allowed to penetrate the full thickness of the core tube wall in order to avoid contaminating the core with oil. The second cut through the remaining thin steel wall was made without lubricant for the milling head. The cores were returned to the laboratory for sampling and lithologic logging. In sampling, no more than half of the core was taken within any sampled interval. After logging and sampling, the remaining core halves were put back together and forced into PVC pipes with end caps sealed airtight with PVC adhesive. It is hoped that further deterioration of the cores will be prevented in this way and the material will be available for future study.

The mineral composition of selected salt samples was determined by X-ray diffraction in the laboratories of the Department of Geology and Geophysics, University of Utah. Preliminary estimates of relative amounts of the various minerals were made by comparison of relative peak heights of the major minerals. Because three different instruments with varying operating conditions and characteristics were used during the course of the study, comparisons of X-ray peak intensities from one machine to another are impossible.

Major element chemical compositions of selected salt samples were determined in the UGMS's analytical laboratory by David Barber, analyst. Standard atomic absorption, gravimetric and colorimetric methods were used. Free water as H₂O (-) was determined by weight loss on drying and the weight percent of water insoluble materials was determined by filtration and weighing. Only the most recent work of the laboratory has been included in this report. Earlier, less accurate analytical work was deleted from the report as unsuitable for publication.

SALT DISTRIBUTION AND THICKNESS

Positions of coring sites in the North Arm of the Great Salt Lake are shown in figure A1. Circles indicate positions occupied by radar fixes on land-based points, triangles indicate points occupied by sextant fixes on land-based points, and squares are used to show points occupied by dead-reckoning methods. The size of the symbols are not meant to imply the error of location. Isopach contours at one foot intervals on figure A1 show the thickness of the salt crust at the time of coring. The longest core taken was a little more than 5 ft (1.4 m) long. Where the salt crust was thickest the cores did not penetrate the salt crust completely and the absolute thickness of the salt crust is not known in these areas. Cores that did penetrate the salt crust are indicated on figure A1 with an asterisk. As will be shown, tonnage estimates based on this isopach map are similar to estimates based on some positional variations of the brines calculated by Whelan (1973) and it seems likely that the isopach contours of figure A1 are therefore reasonably accurate. [*We georeferenced Goodwin's (1973a) maps in ArcMap and the resulting coordinates for the coring locations are presented in table A1. The data presented in tables A1 and A2 are summarized from the cross sections produced by Goodwin; figure A1 shows the locations of points referenced in tables. As indicated by table A1 and as noted above, many of the cores taken did not fully penetrate the salt crust so Goodwin inferred a depth at many of those core sites. We have been unable to determine exactly which cores were taken in 1970 and which were taken in 1972; however, Goodwin did note that sylvite was detected only in cores taken in 1970, suggesting that most of the cores were collected in 1970 (table A3).*]

Two areas of unusually thick salt deposits are shown on figure A1. One, between Gunnison Island on the west and Little Valley on the east, has a maximum salt thickness of at least 4 ft. This southern 4-ft thickness area is not well supported by core information. Cores B-3 and B-4 had core barrels slightly more than 4 ft long, but recovery was very poor and both contained only about 1 ft of core consisting only of salt. Interpretation from surrounding cores, especially A-4 and C-4, seems to require a salt thickness of at least 4 ft near cores B-3 and B-4. The second area of unusually thick salt lies on the line between Dolphin Island and Rozel Point and has salt thickness of at least 5 ft. This thickest area again was not completely penetrated by any core, but control from surrounding cores seems to require a salt thickness of at least 5 ft. It is quite possible that the 4 ft isopach contour is not closed around the 5 ft area and extends southward to include the 4 ft thickness area to the south. If this is the case, the calculated tonnages given below are too low. The interpretation shown on figure A1 seems to be the best one based on all the available information, however.

Bulk Density and Tonnage

Samples from several of the cores were used to determine the bulk density of the salt. To do this, the salt in half of the core tube over a length of 5 cm was carefully extracted to prevent loss of sample. The dry weight of the sample was determined and the diameter of the core tube and length of the sample were used to calculate the volume. Bulk densities determined in this way ranged from 0.612 g/cc to 1.684 g/cc. The computed mean and standard deviation of 17 determinations of density were 1.436 ± 0.181 g/cc. The lowest value (0.612 g/cc) was deleted from the calculation of this mean because all other values were greater than 1 g/cc.

The volume of salt shown in the thickness map (figure A1) was determined by duplicating the map on graph paper and cutting out and weighing the successive half-contour shapes. Although not as accurate as some methods, this method was deemed adequate for the purposes of this report. Using the average density of 1.436 g/cc, the total calculated tonnage of salt in the north arm of the Great Salt Lake is near 1 billion metric tons, in close agreement with the value calculated by Whelan (1973, p. 7) from compositional variations of the brines.

Whelan has shown that the lake reaches halite saturation at a water level elevation of 4195 ft above sea level and will precipitate halite at all elevations below this level. In 1959, just as the railroad causeway was completed, the lake level reached 4195 ft and began precipitating salt (Hahl and Handy, 1969, p. 11). From 1959 to about the end of 1961, the level of the lake continued to fall and salt [*continued*] to precipitate both north and south of the causeway. In February 1966, the water level in the south arm rose above 4195 ft and some dissolution of the salt deposited in the south arm probably began at this time. From 1966 to 1969 there was a net movement of salt northward into the north arm because the north arm remained at or below the water level necessary for halite saturation. After an unusually wet spring season in 1971 the water level in the north arm rose above 4195 ft and salt precipitation in both arms stopped. Since 1971, the total dissolved load in the lake has continued to increase as the salt deposited in the north arm redissolves in the now undersaturated lake (Whelan, 1973; Madison, 1970). From about 1961 on, then, little new salt actually precipitated in the south arm and there was only a net northward movement of salt from south arm to north arm.

SALT COMPOSITION AND LITHOLOGY

Mineralogy

The mineralogy of selected samples was determined by X-ray diffraction techniques. Table A3 lists the results of X-ray analysis and the chemical analyses of the samples. A brief lithologic description is also included. The mineral compositions of table x3 are listed under major and minor minerals. Only one mineral is listed as the major mineral. The minor minerals are listed in order of decreasing abundance as estimated from relative peak heights. Because more than one X-ray diffractometer was used during the course of the study, the X-ray diffractograms of the different instruments are not directly comparable and relative amounts of minerals in one sample compared to another cannot be determined. Because of the exceedingly high X-ray intensities reflected by halite compared to other minerals, the minor minerals present in the samples in amounts less than 5% may have gone completely undetected. In many cases only a few of the most intense X-ray diffraction peaks of minerals other than halite could be detected in the diffractograms.

Table A3 shows that all samples consisting predominantly of crystalline salt are made up almost entirely of halite. Minor minerals in the salt samples are gypsum, sylvite, thenardite and, perhaps, mirabilite. Where oolites were present in the salt or in clays, aragonite was sometimes identified in the diffractograms.

Diffractograms of 1972 core samples commonly showed peaks attributable both to mirabilite and to its anhydrous analog thenardite. Commonly peaks from both minerals were present, but the mirabilite peaks were broad and ill-defined, suggesting that the salt was in varying stages of transition from pure mirabilite to thenardite. Mirabilite is commonly precipitated from the lake brines during the coldest winter months and is re-dissolved during the summer.

Except in a few rare instances, minor minerals in the salt were not directly observed during the lithologic logging of the cores. Gypsum crystals were observed in some of the clay samples from the cores, but mirabilite and thenardite were not. Sylvite was also not observed during lithologic logging. Sylvite was detected by X-ray diffraction only in the cores taken during the summer of 1970. These cores had been stored for up to 18 months before being opened for analysis. Sylvite was not found in any of the 1972 cores that were stored for only 6 months or less before being opened. Sylvite occurs only in limited amounts in the 1970 cores, but its occurrence does not seem to depend on depth beneath the salt surface (see table A3). Two explanations seem possible to explain the almost ubiquitous occurrence of limited amounts of sylvite in the 1970 cores and its absence in the 1972 cores. Firstly, the sylvite may be a secondary mineral that formed during desiccation of the cores while they were stored. Most 1970 cores had crusts of salt around the outsides of the masking tape on the ends of the core tubes and, as discussed below under lithology, the 1972 cores were commonly still damp to the touch whereas the 1970 cores were commonly dry. Secondly, the sylvite could be a primary mineral formed in the salt crust at the time of deposition. Between 1970 and 1972 the sylvite could have been re-dissolved into the lake brines due to the influx of fresh water beginning in 1970. This proposed re-dissolving of sylvite could explain its absence in 1972 cores. The generally high porosity of the salt crust and its relative thinness (less than 4 ft in most areas) makes this solution hypothesis seem plausible. However, the comparative dryness of the 1970 cores compared to the 1972 cores and the fact that the lake brines apparently never reached the saturation composition for sylvite makes the first hypothesis seem much more likely. Slow evaporation of occluded brines in the 1970 cores could easily have caused the brine compositions to reach sylvite saturation and porosities of the salt in the cores was probably high enough to prevent the concentrating of sylvite precipitation near the top and bottom of the core tubes.

Lithology

Salt samples range in grain size from fine needles of halite only a few millimeters long to very coarse cubic crystals up to 1 centimeter on a side. Most salt is in the "medium" grain size range of 2-4 millimeter cubes. Massive, solid beds of salt are very rare. In almost all cases, individual salt cubes could be readily identified and picked out of the core with a spatula or knife. Porosity was estimated visually and for almost all samples was judged to be high (10% or more pore space by volume). Cubes of salt in the 1970 cores commonly were cemented into a hard, interconnected, porous crust that was broken for sampling only with some difficulty. In 1972 cores cementation was much weaker, in general, and the salt was easily broken out for sampling. Some of the 1972 cores still contained brines that could be sucked out of the core with a syringe and most felt damp to the touch. Cores taken in 1970 were uniformly dry to the touch and contained no pockets of fluid brine.

The color of the salt in the cores ranges from clear to white to lavender to a deep rusty grayish brown and all shades in between. Much of the salt, especially in the 1970 cores, is stained a bright yellowish orange. This stain probably came from the corrosion of the galvanized steel core tubes during the 18 months of storage. All 1970 core tubes were strongly corroded on the inside of the core tube. Salt in the 1972 cores was only rarely stained and was commonly clear to white, or stained a dark to medium gray by the presence of inclusions of clay or organic matter.

Sediments beneath the salt crust commonly consist of a very fine-grained, plastic clay. Oolites and gypsum crystals are other common constituents of the clay-rich sediments. Color of the sediments ranges from light gray to a dark olive gray. Bedding was not commonly observed in the sediments, but some samples were finely bedded and were described as, "varved." The clay mineralogy of the sediments was not determined. Some sediment samples were X-rayed after drying. Samples treated in this way commonly showed the presence of abundant halite and other saline minerals. Chemical analyses of sediment samples shown in table A3 indicate far more water extractable sodium, chlorine, sulfate and potassium than would be expected from clay samples not saturated with brines.

Chemical Composition

The major element compositions of selected core samples are shown in table A3. Analyses were performed by standard methods only on the water soluble portions of the samples. Analyses shown in table A3 are those most recently reported by the UGMS's analytical laboratory. Salt samples have been analyzed several times in an attempt to obtain the most accurate analyses possible. These latest results are by far the best analyses yet obtained, although they still have a consistent error that apparently cannot be eliminated even by the most careful analytical methods. None of the chemical analyses shows a perfect balance between the number of moles of positively charged ions and negatively charged ions. As an example of this, table A4 shows a calculation of the moles of (+) and (-) ions from analysis number 5105 of table A3, after recalculating to 100%. This analysis shows the closest approach to 100% total of all of the analyses in table A3. If the moles of (+) charge are summed and subtracted from the sum of the moles of (-) charge, a 0.0005 mole excess of (-) charge appears. This is the smallest difference between charges that has been observed. For all other analyses, the difference is greater than this value. For all analyses shown in table A3, the average difference between moles of charge is 0.083 excess moles of (-) charge [*Goodwin cites an appendix I here, which we have been unable to locate*]. This means that any calculated mineral analyses based on the chemical analyses will inevitably produce a small amount of leftover ions that cannot be accounted for in any mineral composition. A rational mineral analysis calculated from the data of table A4 is shown in table A5.

Table A6 shows the mean and standard deviations of the chemical analyses of 46 salt samples from table A3. Analyses with lithologies other than pure salt were not included in the calculation. The difference in the sums of charges in the average analysis of table A6 indicates an excess of negative charge of 0.063 moles. This clearly indicates that there is a consistent error in the analyses. [*Goodwin cites appendix I here again*] shows that for all the analyses, only a few show any excess of positive charge. If there were only a random variation in the analyses, the difference in moles of charge for the average analysis should much more closely approach 0 than it does.

Table A7 shows an average brine analysis for surface north arm brines. The average analysis was calculated from analyses of brines collected in November of 1971 (UGMS page number 491C-130). This average brine analysis also shows an excess of 0.131 moles of (-) charge over (+) charge. Thus, it is not just the solid salt analyses that show this consistent error.

From the available data, the source of the error cannot be directly determined. There could be a consistent deficiency of positive ions, or a consistent excess of negative ions, or a combination of the two. The most likely source of error is in the gravimetric determinations of SO_4 by precipitation with BaCl_2 . Until these analytical problems can be eliminated, rational analyses calculated from the brine analyses and from salt analyses have little value. Agreement should be within ± 0.002 moles of charge for this is near the probable range of error in the weight percent of the major ions present in smaller amounts.

CONCLUSIONS

A salt crust deposited in the northern end of the Great Salt Lake, Utah, between 1959 and 1971 is more than 5 ft thick at its greatest thickness. Core samples of the salt crust taken in 1970 and 1972 show that the salt consists of a moderately cemented, porous network of cubic salt crystals ranging from a few millimeters up to 1 centimeter on a side. Except near the shores of the lake, little sediment is mixed with the salt. The salt bed consists almost entirely of pure halite. Most samples of the salt contain minor amounts of thenardite (Na_2SO_4) and some partially altered and dehydrated mirabilite ($\text{Na}_2\text{SO}_4 \cdot 10\text{H}_2\text{O}$). The total tonnage of salt deposited in the north arm is near 1 billion metric tons, based on an average bulk density of the salt of 1.436 g/cc determined from volumetric samples of the cores. The latest analyses of the salt and brines performed by the analytical laboratory of the UGMS show a consistent bias toward an excess of negative ions over positive ions.

REFERENCES CITED

- Hahl, D.C., and Handy, A.H., 1969, Great Salt Lake, Utah—chemical and physical variations of the brine, 1963-1966: Utah Geological and Mineralogical Survey Water Resources Bulletin 12, 33 p.
- Madison, R.J., 1970, Effects of a causeway on the chemistry of the brine in Great Salt Lake, Utah: Utah Geological and Mineralogical Survey Water Resources Bulletin 14, 52 p.
- Whelan, J.A., 1973, Great Salt Lake, Utah—chemical and physical variations of the brine, 1966-1972: Utah Geological and Mineralogical Survey Water Resources Bulletin 17, 24 p.

Table A1. Maximum measured salt thickness and estimated salt crust base from Goodwin (1973a).

Data Point	Measured Salt Thickness ¹ (feet)	Inferred Salt Crust Thickness ¹ (feet)	Measured Salt Thickness (?) ² (feet)	UTM Coordinates ³ Z12, NAD83	
				Easting (m)	Northing (m)
A-4	no data	no data	3.4	358409	4566001
B-2	2.35	not projected	2.3	365374	4570292
B-3	0.90	not projected	4.0	360838	4570279
B-4	1.35	not projected	4.0	356635	4570306
B-5	no data	no data	2.4	351080	4568991
C-2	no data	no data	3.1	369289	4574566
C-3	3.00	3.20	3.0	363935	4575066
C-4	2.85	3.00	4.0	358749	4574834
C-5	2.00	3.00	3.0	354741	4574894
C-6	2.10	2.40	1.8	350369	4574451
D-1	0.00	0.00	0.0	370723	4579239
D-2	3.00	3.00	3.1	366385	4579945
D-3	1.95	3.40	2.9	362406	4580072
D-4	2.30	3.20	3.1	357126	4580086
D-5	no data	no data	3.4	352696	4578915
D-6	2.40	2.40	2.3	349546	4580363
E-1	0.00	0.00	0.0	368399	4583905
E-2	0.00	0.00	0.0	364637	4584799
E-3	1.75	3.60	1.8	359723	4585651
E-4	3.70	4.80	4.7	355325	4585977
E-5	4.60	4.90	4.6	350134	4585244
E-6	2.75	4.35	4.3	345059	4584954
E-7	3.70	3.70	3.7	340455	4585144
F-1	1.20	1.45	1.4	358227	4589011
F-2	4.35	5.00	4.2	353351	4588968
F-3	4.10	5.00	4.1	349554	4589960
F-4	no data	no data	1.6	343979	4588520
F-5	no data	no data	2.0	339586	4588085
G-1	1.70	2.50	2.0	353718	4594675
G-2	3.80	4.00	3.9	352083	4593723
G-3	3.30	3.30	3.3	344693	4595744
G-4	1.10	2.20	1.2	337254	4596031
I-2	no data	no data	2.3	344649	4603725

¹Data from Goodwin's cross sections.

²Data from Goodwin's salt isopach map. Definition of this number is not specified on map, but likely represents measured salt thickness.

Discrepancies exist between cross sections and the isopach map.

³Coordinates were digitized from the salt isopach and core location maps and are very approximate.

Table A2. Cross-section data from Goodwin (1973a).

Data Point	From (feet)	To (feet)	Thickness (feet)	Base of Salt	
				Intercepted?	Goodwin's Description
B-2	0.00	2.35	2.35	No	massive crystalline salt
B-3	0.00	0.90	0.90	No	massive crystalline salt
B-4	0.00	1.35	1.35	No	massive crystalline salt
C-3	0.00	3.00	3.00	No	massive crystalline salt
C-4	0.00	2.75	2.75		massive crystalline salt
C-4	2.75	2.85	0.10	No	mixed massive crystalline salt and fine-grained silt or clay
C-5	0.00	2.00	2.00	No	massive crystalline salt
C-6	0.00	2.10	2.10	Yes	massive crystalline salt
C-6	2.10	2.40	0.30		oolitic sand and silt and disseminated crystals of salt
D-1	0.00	0.00	0.00		<i>no salt</i>
D-2	0.00	2.85	2.85		massive crystalline salt
D-2	2.85	3.00	0.15	Yes	mixed massive crystalline salt, fecal pellets or other organic material, and fine-grained silt or clay
D-3	0.00	1.00	1.00		massive crystalline salt
D-3	1.00	1.50	0.50		lost core
D-3	1.50	2.45	0.95	No	massive crystalline salt
D-4	0.00	0.55	0.55		massive crystalline salt
D-4	0.55	1.75	1.20		mixed massive crystalline salt and fecal pellets or other organic material
D-4	1.75	2.50	0.75		lost core
D-4	2.50	3.05	0.55	No	massive crystalline salt
D-6	0.00	2.00	2.00		massive crystalline salt
D-6	2.00	2.40	0.40	Yes	mixed massive crystalline salt, fecal pellets or other organic material, and fine-grained silt or clay
E-1	0.00	0.00	0.00		<i>no salt</i>
E-2	0.00	0.00	0.00		<i>no salt</i>
E-3	0.00	1.75	1.75	No	massive crystalline salt
E-4	0.00	3.70	3.70	No	massive crystalline salt
E-5	0.00	4.60	4.60	No	massive crystalline salt
E-6	0.00	2.75	2.75	No	massive crystalline salt
E-7	0.00	3.70	3.70	Yes	massive crystalline salt
F-1	0.00	0.65	0.65		massive crystalline salt
F-1	0.65	0.90	0.25		mixed oolitic sand and silt and fine-grained silt and clay
F-1	0.90	1.45	0.55	Yes	massive crystalline salt
F-2	0.00	4.35	4.35	No	massive crystalline salt
F-3	0.00	4.10	4.10	No	massive crystalline salt
G-1	0.00	0.40	0.40		massive crystalline salt (<i>unclear what represents base of salt crust - this study</i>)
G-1	0.40	0.50	0.10		oolitic sand and silt
G-1	0.50	0.60	0.10		mixed massive crystalline salt and oolitic sand and silt
G-1	0.60	1.10	0.50		mixed oolitic sand and silt and fine-grained silt and clay
G-1	1.10	1.35	0.25		massive crystalline salt
G-1	1.35	1.50	0.15		mixed massive crystalline salt and oolitic sand and silt
G-1	1.50	1.80	0.30		mixed massive crystalline salt, oolitic sand and silt, and fine-grained silt and clay
G-1	1.80	2.00	0.20		mixed oolitic sand and silt and fine-grained silt and clay
G-1	2.00	2.30	0.30		mixed massive crystalline salt and fine-grained silt and clay
G-1	2.30	2.45	0.15		mixed massive crystalline salt and oolitic sand and silt
G-1	2.45	2.50	0.05	Yes (?)	massive crystalline salt
G-2	0.00	3.80	3.80	No	massive crystalline salt
G-3	0.00	0.90	0.90		massive crystalline salt
G-3	0.90	1.80	0.90		mixed massive crystalline salt and fecal pellets or other organic material
G-3	1.80	3.30	1.50	Yes	mixed massive crystalline salt and globular masses of salt or grapestone (?)

Table A3. Chemical analyses, mineralogical analyses and lithologic descriptions of selected samples from cores of the salt crust in the north arm of the Great Salt Lake, Utah. Mineral abbreviations are H = halite; S = sylvite; A = aragonite; G = gypsum; T = thenardite; M = mirabilite; M-T = peaks of both M and T present suggesting an intermediate phase of unknown composition and structure. Parentheses indicated minerals present in only minor amounts and identified in X-ray diffractograms from only 1 or 2 major peaks. Minor minerals are listed in decreasing order of abundance from left to right.

Lab no.	Core no.	Interval	Cl	SO ₄	Na	K	Ca	Mg	Fe	H ₂ O	Insolubles	Total	Major Mineral	Minor Mineral	Lithology
4931	A-4	32-37	46.81	15.73	35.9	0.38	0.24	0.2	<2	n.d.	0.06	99.32	H	T(M)	very coarse salt
4932	A-4	37-40	54.46	4.43	37.1	0.34	0.4	0.12	<2	n.d.	2.91	99.76	H	M-T, G	med. to coarse salt
4934	B-4	0-6	51.03	8.78	36.2	0.07	0.22	0.03	<2	n.d.	3.42	99.75	H	S,T	fine to medium salt
4939	G-3	29-32	59.22	0.86	38.2	0.18	0.34	0.04	<2	n.d.	0.36	99.2	H	G, M-T	fine to med. salt w/ abdt. shrimp egg
5077	D-4	0-7	59.49	0.68	38.86	0.15	0.13	0.1	<1	0.05	0.1	99.56	H	S,T	fine to medium salt
5078	D-4	16-17.5	59.47	0.6	38.74	0.16	0.14	0.12	<1	0.06	0.24	99.53	H	S	med. to coarse salt
5079	D-4	17.5-18.5	59.77	0.63	38.61	0.28	0.13	0.19	<1	0.15	0.17	99.93	H	S,G	fine to med. salt
5080	D-4	213/4-30	59.57	0.98	38.3	0.21	0.13	0.16	<1	0.05	0.26	99.66	H	S	fine to med. salt
5081	D-5	3-6	57.9	1.57	36.89	0.28	0.41	0.16	<1	1.18	1.5	99.89	H	G, M-T	fine to med. salt
5085	D-6	30.5	10.39	1.98	9.89	0.07	1.29	0.6	<1	3.23	72.31	99.75	H	S	
5086	D-4	30-37	43.97	4.77	19.92	0.33	2.57	0.29	<1	2.98	25	99.83	H	S, T	fine to med. salt
5087	E-1	0-3	59.42	0.15	37.37	0.15	0.31	0.1	<1	0.44	1.87	99.83	H	S	fine to med. salt
5088	E-1	13-15	60.2	0.73	37.57	0.26	0.15	0.18	<1	0.47	0.32	99.81	H	S	fine to med. salt
5089	E-1	24-30	10.05	1.41	9.39	0.27	0.41	0.29	<1	3.38	74.15	99.35	G	H	pale olive gray, fine clay
5090	E-1	38	8.6	0.95	4.64	0.18	0.23	0.17	<1	2.18	82.87	99.82	H	S	pale olive gray, fine clay
5091	E-1	45	4.92	10.12	2.35	0.09	3.36	0.2	<1	5.52	73.29	99.85	H	S	pale olive gray, fine clay and gyps.
5092	E-2	3.5	8.44	1.02	5.02	0.27	0.29	0.31	<1	3.35	80.96	99.66	n.d.	n.d.	light gray, fine clay
5093	E-2	11	16.74	1.15	8.81	0.37	0.28	0.36	<1	3.02	69.02	99.75	n.d.	n.d.	olive gray, varved, fine clay
5094	E-2	14	17.85	2.21	9.25	0.34	0.96	0.31	<1	2.95	65.88	99.75	n.d.	n.d.	med. to dark gray clay and fecal pels
5095	E-2	16.5	5.39	1.17	2.47	0.16	0.3	0.24	<1	2.59	87.56	99.88	n.d.	n.d.	light to olive gray, fine clay
5096	E-2	24.5	6.39	1.01	2.96	0.06	0.57	0.29	<1	2.45	86.02	99.75	H	S,G	light gray to very light gray clay
5097	E-2	36.4	60	0.08	38.7	0.13	0.07	0.09	<1	0.31	1.26	100.64	H	S	fine to med. salt bed in clay
5098	E-2	50	8.99	1.63	6.39	0.32	0.35	0.42	<1	3.17	78.56	99.83	H	S, M-T	light gray, fine clay
5100	E-2	44-45	49.29	7.42	26.54	3.02	0.12	3.1	<1	8.89	1.37	99.73	H	A, G	mixed salt and clay
5101	E-3	0-2.5	12.31	2.33	10.31	0.4	0.62	0.34	<1	11.3	62.03	99.64	H	S	mixed salt and clay
5102	E-4	1	59.2	0.3	38.6	0.07	0.13	0.03	<1	0.18	1.22	99.73	H	S	coarse to med. salt
5103	E-4	17.5	58.4	0.08	37.48	0.12	0.06	0.04	<1	0.41	3.32	99.91	H	S, (G)	coarse to massive salt
5104	E-4	34	59.59	0.96	38.13	0.08	0.31	0.04	<1	0.37	0.27	99.75	H	S	coarse to very coarse salt
5105	E-4	45-48	60.26	0.29	38.91	0.07	0.07	0.03	<1	0.2	0.13	99.96	H	M-T	coarse to very coarse salt
5106	E-5	0.1	59.6	1.37	38	0.11	0.2	0.1	<1	0.55	0.05	99.88	n.d.	n.d.	medium salt
5107	E-6	6-9	60.2	0.32	38.89	0.05	0.1	0.05	<1	0.23	0.23	100.07	n.d.	n.d.	coarse to medium salt
5108	E-5	12-18	59.5	1.37	38	0.12	0.17	0.1	<1	0.5	0.13	99.89	H	S	medium to coarse salt

Table A3. Continued.

Lab no.	Core no.	Interval	Cl	SO ₄	Na	K	Ca	Mg	Fe	H ₂ O	Insolubles	Total	Major Mineral	Minor Mineral	Lithology
5109	E-5	26-30	60.04	0.51	38.7	0.06	0.16	0.07	<1	0.23	0.12	99.89	H	S, G	medium to coarse salt
5110	E-5	50-55	60.17	0.5	38.4	0.05	0.16	0.03	<1	0.24	0.2	99.75	H	S	coarse to very coarse salt
5111	E-6	0-10.5	59.7	0.73	38	0.23	0.15	0.22	<1	0.17	0.62	99.82	H	M-T	coarse to medium salt
5112	E-6	10.5-13.25	60	0.14	38.7	0.08	0.04	0.05	<1	0.34	0.36	99.71	n.d.	n.d.	coarse to medium salt
5113	E-6	16-18	59.3	1.12	38	0.23	0.25	0.18	<1	0.17	0.12	99.37	H	G, M-T	coarse to medium salt
5114	E-6	21-23	60	0.13	38.7	0.06	0.12	0.04	<1	0.21	0.54	99.8	H	A, G	medium to fine salt
5115	E-6	38-40	7.35	1.19	4.96	0.28	0.27	0.34	<1	3.12	82.16	99.67	H	T(?)	gray, fine clay and oolites
5116	E-7	0-3.5	7.51	1.33	4.82	0.26	0.32	0.3	<1	3.17	82	99.71	H	A, G, T	light, gray green clay and oolites
5117	E-7	3.5-14.5	7.89	2.19	5.03	0.34	0.52	0.4	<1	2.79	80.43	99.59	H	A, G, T	medium to dark gray clay and oolites
5120	E-7	27.5-37	60	0.52	38.5	0.35	0.16	0.05	<1	0.21	0.26	100.05	H	S, (T)	fine to medium salt
5121	E-7	37.5-43.5	60.26	0.53	38.1	0.34	0.18	0.02	<1	0.11	0.32	99.86	H	S	coarse to medium salt
5122	E-7	43.5-48	60.02	0.47	38.68	0.34	0.15	0.02	<1	0.09	0.15	99.92	H	S, (T)	coarse to medium salt
5123	E-7	48-59	60.17	0.3	38.3	0.37	0.08	0.03	<1	0.1	0.27	99.62	H	S	salt ranging from coarse to needles
5132	F-2	0-3	15.9	1.59	4.28	0.65	0.36	0.5	<1	2.36	71.15	96.79	H	S	light gray, fine clay
5133	F-2	9-11	57.58	1.74	36.8	0.34	0.16	0.04	<1	0.1	3.04	99.8	H	S	medium to coarse salt
5134	F-2	15-31	60.35	0.75	38.06	0.04	0.13	0.03	<1	0.08	0.14	99.58	H	S	medium to coarse salt
5135	F-2	33-43	58.69	0.41	36.68	0.41	0.18	0.02	<1	0.16	3.27	99.82	H	S	medium to coarse salt
5136	F-3	0-6	60.33	0.16	38.52	0.41	0.11	0.01	<1	0.16	0.17	99.87	H	S	coarse to medium salt
5137	F-3	20-24	58.32	2.69	36.45	0.67	0.36	0.25	<1	0.59	0.46	99.79	H	S	coarse to medium salt
5138	F-3	37-41	59.4	1.42	36.04	0.62	0.36	0.18	<1	0.51	1.26	99.79	H	S	fine to medium salt
5139	F-4	3-6	60.13	0.54	37.06	0.7	0.41	0.03	<1	0.39	0.54	99.8	H	M-T	medium salt
5140	F-4	15-18	60.25	0.67	37.03	0.52	0.1	0.14	<1	0.65	0.36	99.72	H	G, M-T	medium salt
5141	F-5	0-3	60.2	0.53	37.51	0.52	0.13	0.1	<1	0.39	0.33	99.71	H	G, M-T	coarse
5142	F-5	26-32	34.96	11.97	19.66	0.33	2.54	0.15	<1	7.7	22.51	99.82	H	A	silty clay with salt
5143	F-5	51-51.5	12.13	1.26	3.34	0.49	0.41	0.29	<1	2.02	79.79	99.73	A	H	fine clay
5144	F-5	55.88	12.35	1.23	3.49	0.45	0.34	0.3	<1	2.29	79.36	99.81	H	(M-T)	fine clay
5145	F-5	59-63	34.46	2.97	9.09	1.46	0.91	0.62	<1	17.63	32.44	99.58	H	(M-T)	vine clay
5146	G-1	0-1	17.43	1.64	5.39	0.73	0.65	0.29	<1	15.52	58.06	99.71	H	S	
5147	G-1	1-2.5	60.09	0.19	36.69	0.36	0.27	0.08	<1	0.33	1.25	99.26	H	S, A, (G)	alternating beds of oolite and salt
5148	G-1	2.5-6.5	74.36	1.57	21.1	0.41	0.89	0.11	<1	1.39	0.11	99.94	H	S	coarse salt
5149	G-3	18-20	59.59	0.28	35.39	0.49	0.49	0.13	<1	0.82	2.54	99.73	H	M-T	coarse to med. salt
5150	G-3	29-32	60	0.46	35.24	0.33	0.2	0.03	<1	0.28	3.17	99.71	H	M-T	coarse to med. salt
5151	G-3	51-53	60.02	0.11	36.18	0.29	0.12	0.03	<1	0.17	2.87	99.79	H	M-T	coarse to med. salt
5152	I-2	36-38	60.09	0.32	37.22	0.33	0.21	0.06	<1	0.28	1.15	99.66	H	G, M-T	fine to med. salt
5153	I-2 (?)	15.5-19	60.15	0.87	36.62	0.38	0.23	0.14	<1	0.4	1.06	99.85	n.d.	n.d.	fine to medium to coarse salt

Note: Table reproduced without change from Goodwin (1973a)

B-2 (?)

Table A4. Chemical analysis of salt sample 5105 from table A3. Analysis is recalculated to total 100%. Moles of major elements and moles of charge are shown.

Element	Weight %	moles of element	moles of charge
Cl	60.28	1.700	1.700
SO ₄	0.29	0.003	0.006
Na	38.93	1.693	1.693
K	0.07	0.002	0.002
Ca	0.07	0.002	0.004
Mg	0.03	0.002	0.002
H ₂ O	0.20		(-) = 1.706
water insoluble	0.13		(+) = 1.701
Total	100.00		0.005 (-)

Note: Table reproduced without change from Goodwin (1973a)

Table A5. Rational mineral analysis calculated from the data of above table A4. Note that the excess of Cl left over below corresponds to the excess moles of (-) ions shown in above table A4.

Compound	Number of moles
CaSO ₄	0.002
Na ₂ SO ₄	0.001
KCl	0.002
MgCl ₂	0.001
NaCl	1.691
Cl remaining	0.005

Note: Table reproduced without change from Goodwin (1973a)

Table A6. Average chemical analysis of 46 salt samples from cores of the north arm salt crust. Values are in weight percent. An analysis recalculated to 100% total is also shown and the moles of the ions calculated from that analysis. Standard deviations are shown for the average values.

Element	Weight %	Recalculated Wt. %	Moles of Ions
Cl	59.07 ± 8.45	59.16	1.700
SO ₄	1.36 ± 2.65	1.36	0.006
Na	36.89 ± 3.67	36.94	1.693
K	0.28 ± 0.16	0.28	0.002
Ca	0.26 ± 0.38	0.26	0.004
Mg	0.10 ± 0.07	0.10	0.002
H ₂ O (-)	0.40 ± 0.49	0.40	(-) = 1.697
Insol. in water	1.50 ± 13.66	1.50	(+) = 1.634
Total	99.86	100.00	

Note: Table reproduced without change from Goodwin (1973a)

Table A7. Average chemical analysis of surface brines, north arm, Great Salt Lake, Utah. Brines are from the November, 1971 sampling and are the 0 feet and 5 feet samples from UGMS brine analysis sheet number 491C-130. Field densities were used to recalculate the analysis from gm/liter to gm/1000gm brine.

Element	gm/1000 gm brine	moles/1000 gm brine
Cl	141.914 ± 3.522	4.003
SO ₄	21.628 ± 0.626	0.225
Na	74.170 ± 2.535	3.226
K	7.880 ± 0.508	0.202
Ca	0.123 ± 0.027	0.003
Mg	10.785 ± 0.358	0.444
		(-) = 4.453
		(+) = 4.322

Note: Table reproduced without change from Goodwin (1973a)

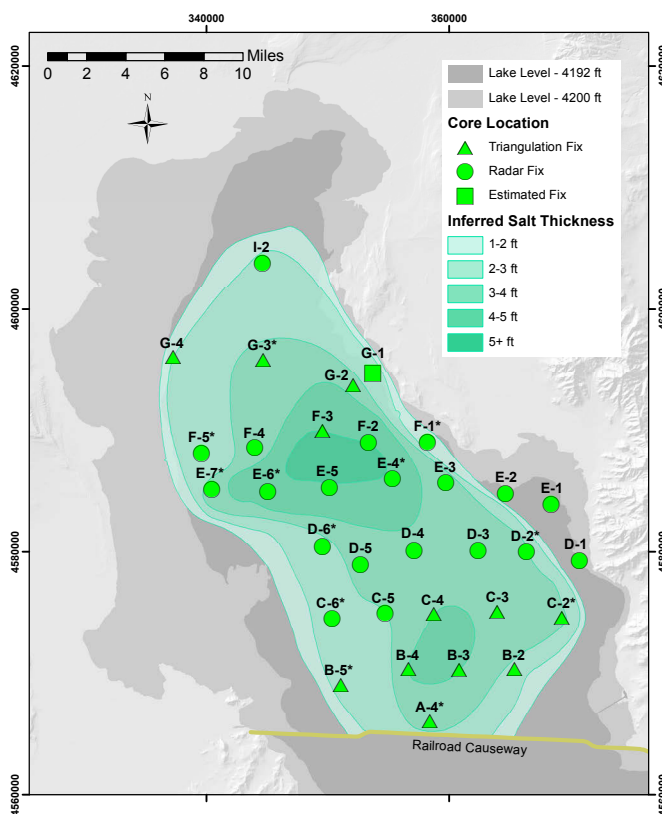


Figure A1. Salt isopach map and data points from Goodwin (1973a). Relevant information for data points are presented in tables A1 and A2. * indicates cores that completely penetrated the salt crust. Lake levels are based on bathymetry from Baskin and Allen (2005) and Baskin and Turner (2006). Coordinates are UTM Z12 NAD83.

Appendix B Supplementary Photographs



Figure B1. Battery-powered 18v Milwaukee SDS plus rotary hammer (Cat. No. 2715-20).



Figure B2. SDS plus, 37-inch-long (39 inches with shank), 3/4-inch-diameter masonry bit.



Figure B3. SDS plus to SDS plus extension, 18 inches long. Extension is manufactured by the Relton Corporation.

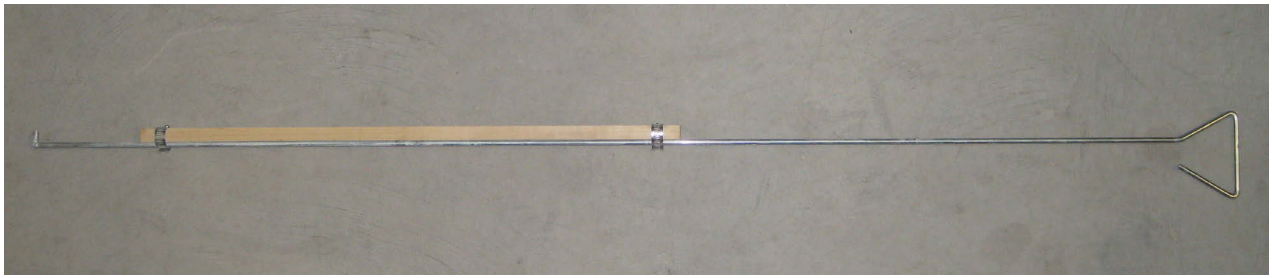


Figure B4. Fabricated caliper for measuring salt thickness. Total length of device is 4.5 ft.



Figure B5. Measuring end of caliper.



Figure B6. Excavation site for sample SCI 1. Gray debris is oolitic sand and mud from below salt crust. Sample block is shown on right.



Figure B7. Excavation site for sample SCI 1. Gray debris is oolitic sand and mud from below salt crust. Sample block is shown on right.

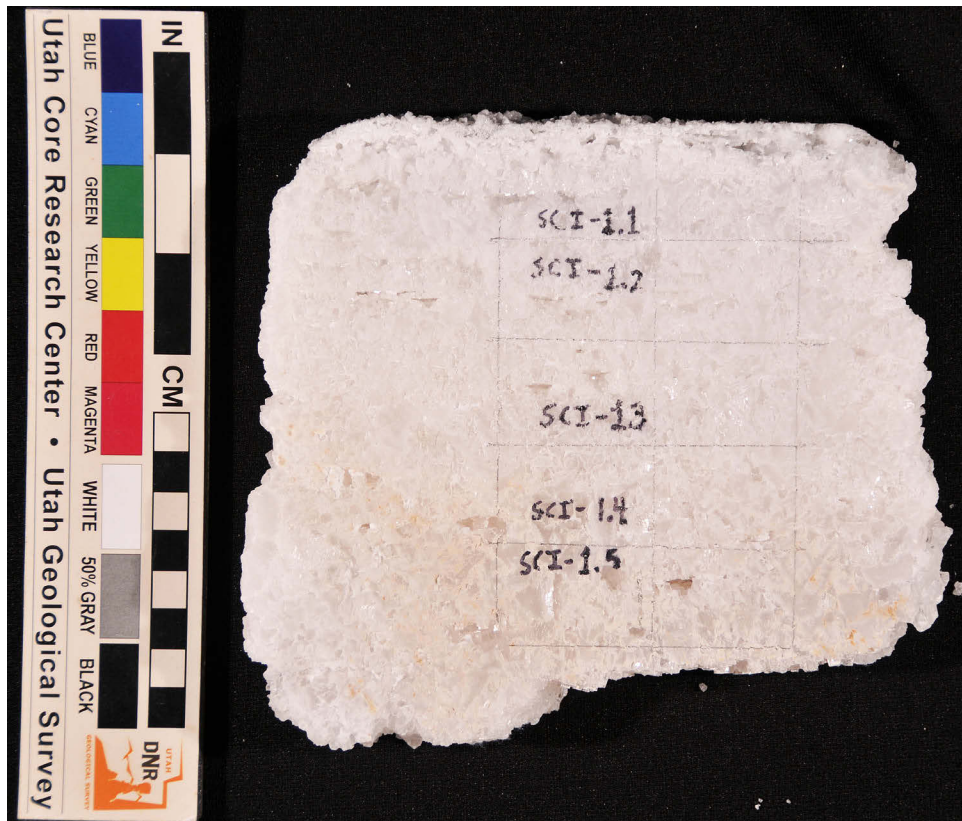


Figure B8. Sample horizon locations from sample SCI 1. Cut surface.

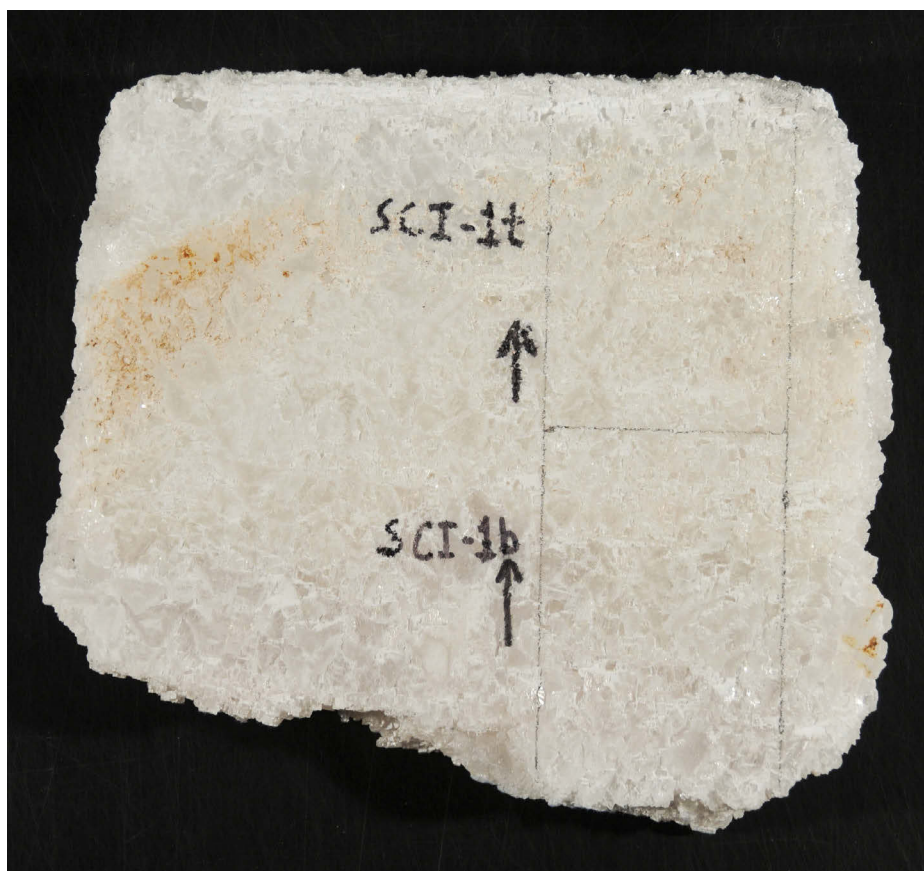


Figure B9. Sample SCI 1 thin section locations. Arrows indicate direction of top of sample. Cut surface.



Figure B10. Fragment of sample SCI 2. Reflective areas are salt rafts from within the salt crust that were exposed when sample was broken open. Pen is 5.6 inches long.



Figure B11. Rough, uncut surface of sample SCI 2. Subtle horizontal linear features in lower half of sample likely represent past accumulations of salt rafts.

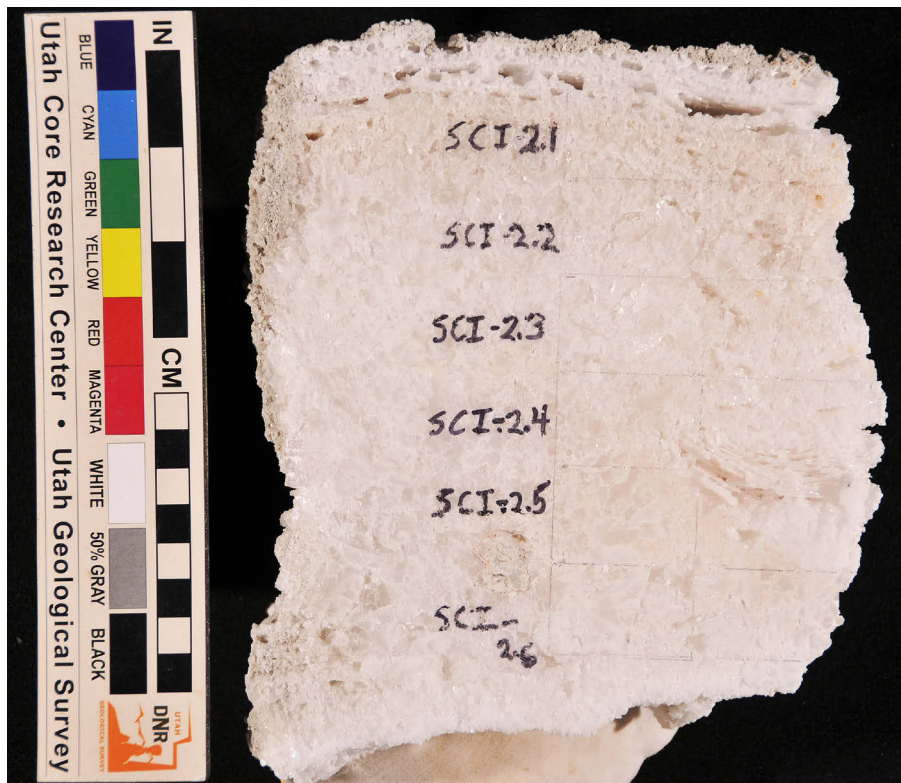


Figure B12. Sample horizon locations from sample SCI 2. Cut surface.

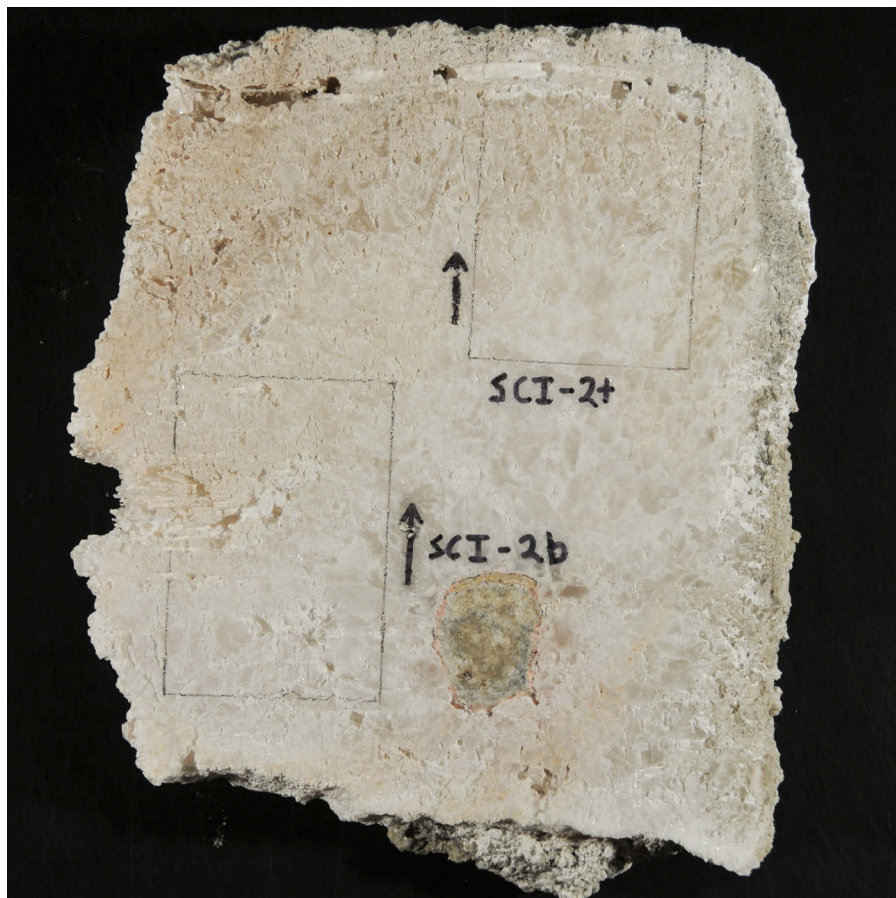


Figure B13. Sample SCI 2 thin section locations. Arrows indicate direction of top of sample. Cut surface.

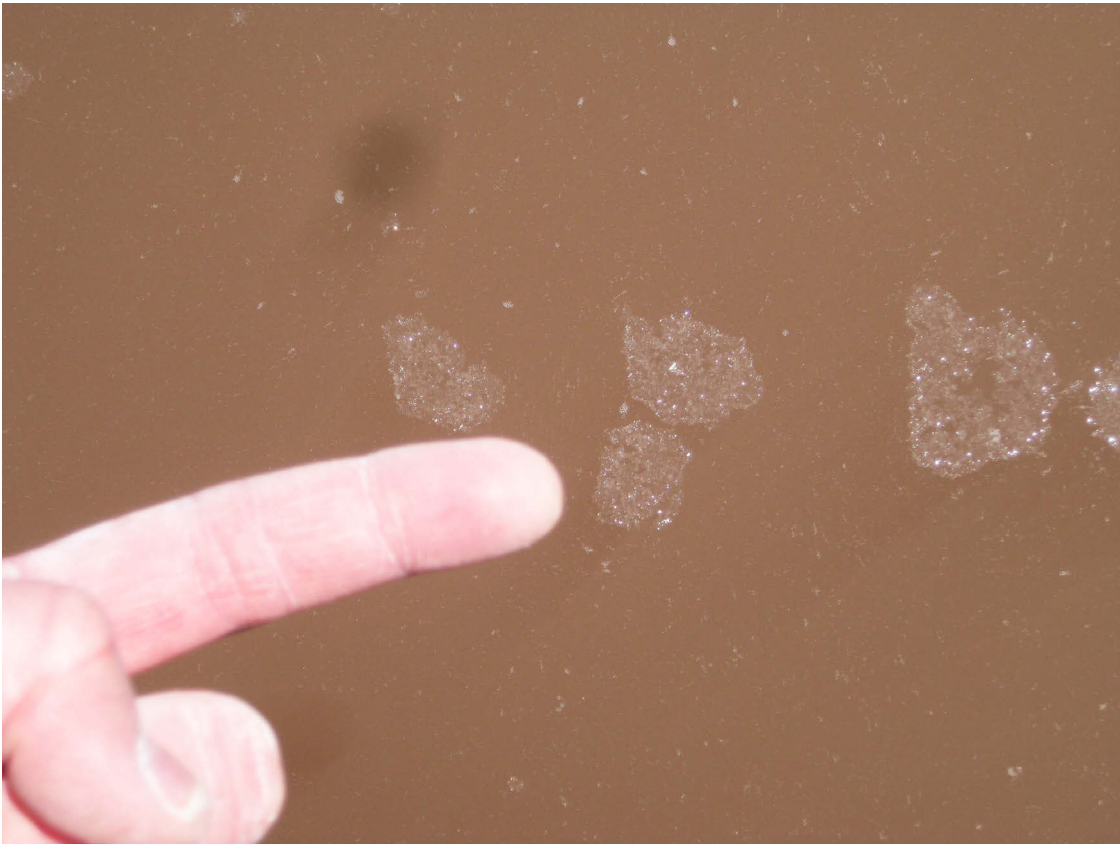


Figure B14. Salt rafts forming on the surface of the brine in the north arm of GSL.



Figure B15. Salt rafts forming on the surface of the brine in the north arm of GSL.



Figure B16. Older coarsely crystalline salt (pink) overlain by more recently precipitated fine-grained salt (white). Gray areas represent a thin veneer of oolitic sand and mud between salt layers. East shore of north arm near transect 6.



Figure B17. Dissolution of exposed salt crust. East shore of north arm near transect 4. Dark gray areas represent oolitic sand and mud exposed from dissolution of salt.



Figure B18. Microbialite mounds are abundant along transect 7. The microbialite mounds are capped by a thin salt crust that also fills the areas in between the mounds. Drilling suggests that many microbialite mounds are also present beneath salt crust.

Appendix C Sample Data

Table C1. Salt crust sample locations.

Sample No.	UTM, Z12 NAD83		Location Comment
	Easting (m)	Northing (m)	
SCI 1	359999	4588525	Spiral Jetty, transect 2
SCI 2	371546	4569664	Promontory Point, transect 7
SCI 3	337577	4593173	West side of Gunnison Bay, transect 8

Table C2. Salt crust full elemental analytical results.

Sample No.	Br Anions	Cl Anions	Ag Soluble	Al ₂ O ₃ Soluble	Ba Soluble	Be Soluble	CaO Soluble	Cd Soluble
	wt. %	wt. %	ppm	wt. %	ppm	ppm	wt. %	ppm
SCI 1.2	0.002	59.6	<0.2	<0.01	<1	<0.2	0.04	<1
SCI 1.4	0.002	59.6	<0.2	<0.01	<1	<0.2	0.30	<1
SCI 2.2	0.002	59.5	<0.2	<0.01	<1	<0.2	0.40	<1
SCI 2.4	0.002	60.0	<0.2	<0.01	<1	<0.2	0.07	<1
SCI 3	0.002	60.1	<0.2	<0.01	<1	<0.2	0.07	<1
SCI 3 R	0.002	59.8	<0.2	<0.01	<1	<0.2	0.07	<1

Sample No.	Ce Soluble	Co Soluble	Cr Soluble	Cu Soluble	Dy Soluble	Er Soluble	Eu Soluble	Fe ₂ O ₃ Soluble
	ppm	wt. %						
SCI 1.2	<1	<1	<1	<1	<0.2	<0.2	<0.2	<0.01
SCI 1.4	<1	<1	<1	<1	<0.2	<0.2	<0.2	<0.01
SCI 2.2	<1	<1	<1	<1	<0.2	<0.2	<0.2	<0.01
SCI 2.4	<1	<1	<1	<1	<0.2	<0.2	<0.2	<0.01
SCI 3	<1	<1	<1	<1	<0.2	<0.2	<0.2	<0.01
SCI 3 R	<1	<1	<1	<1	<0.2	<0.2	<0.2	<0.01

Sample No.	Ga Soluble	Gd Soluble	Hf Soluble	Ho Soluble	K ₂ O Soluble	La Soluble	Li Soluble	MgO Soluble
	ppm	ppm	ppm	ppm	wt. %	ppm	ppm	wt. %
SCI 1.2	<1	<1	<1	<1	0.18	<1	1	0.05
SCI 1.4	<1	<1	<1	<1	0.05	<1	1	0.05
SCI 2.2	<1	<1	<1	<1	0.03	<1	1	0.06
SCI 2.4	<1	<1	<1	<1	0.02	<1	1	0.06
SCI 3	<1	<1	<1	<1	<0.01	<1	<1	0.01
SCI 3 R	<1	<1	<1	<1	<0.01	<1	<1	0.01

Table C2. Continued.

Sample No.	MnO Soluble wt. %	Mo Soluble ppm	Na₂O Soluble wt. %	Nb Soluble ppm	Nd Soluble ppm	Ni Soluble ppm	P₂O₅ Soluble wt. %	Pb Soluble ppm
SCI 1.2	<0.01	<1	52.8	<1	<1	<1	<0.01	<1
SCI 1.4	<0.01	<1	52.6	<1	<1	<1	<0.01	<1
SCI 2.2	<0.01	<1	52.6	<1	<1	<1	<0.01	<1
SCI 2.4	<0.01	<1	53.2	<1	<1	<1	<0.01	<1
SCI 3	<0.01	<1	53.2	<1	<1	<1	<0.01	<1
SCI 3 R	<0.01	<1	53.0	<1	<1	<1	<0.01	<1

Sample No.	Pr Soluble ppm	S Soluble ppm	Sc Soluble ppm	Sm Soluble ppm	Sn Soluble ppm	Sr Soluble ppm	Ta Soluble ppm	Tb Soluble ppm
SCI 1.2	<1	428	<1	<1	<1	<1	<1	<1
SCI 1.4	<1	1910	<1	<1	<1	3	<1	<1
SCI 2.2	<1	2550	<1	<1	<1	4	<1	<1
SCI 2.4	<1	642	<1	<1	<1	<1	<1	<1
SCI 3	<1	416	<1	<1	<1	<1	<1	<1
SCI 3 R	<1	415	<1	<1	<1	1	<1	<1

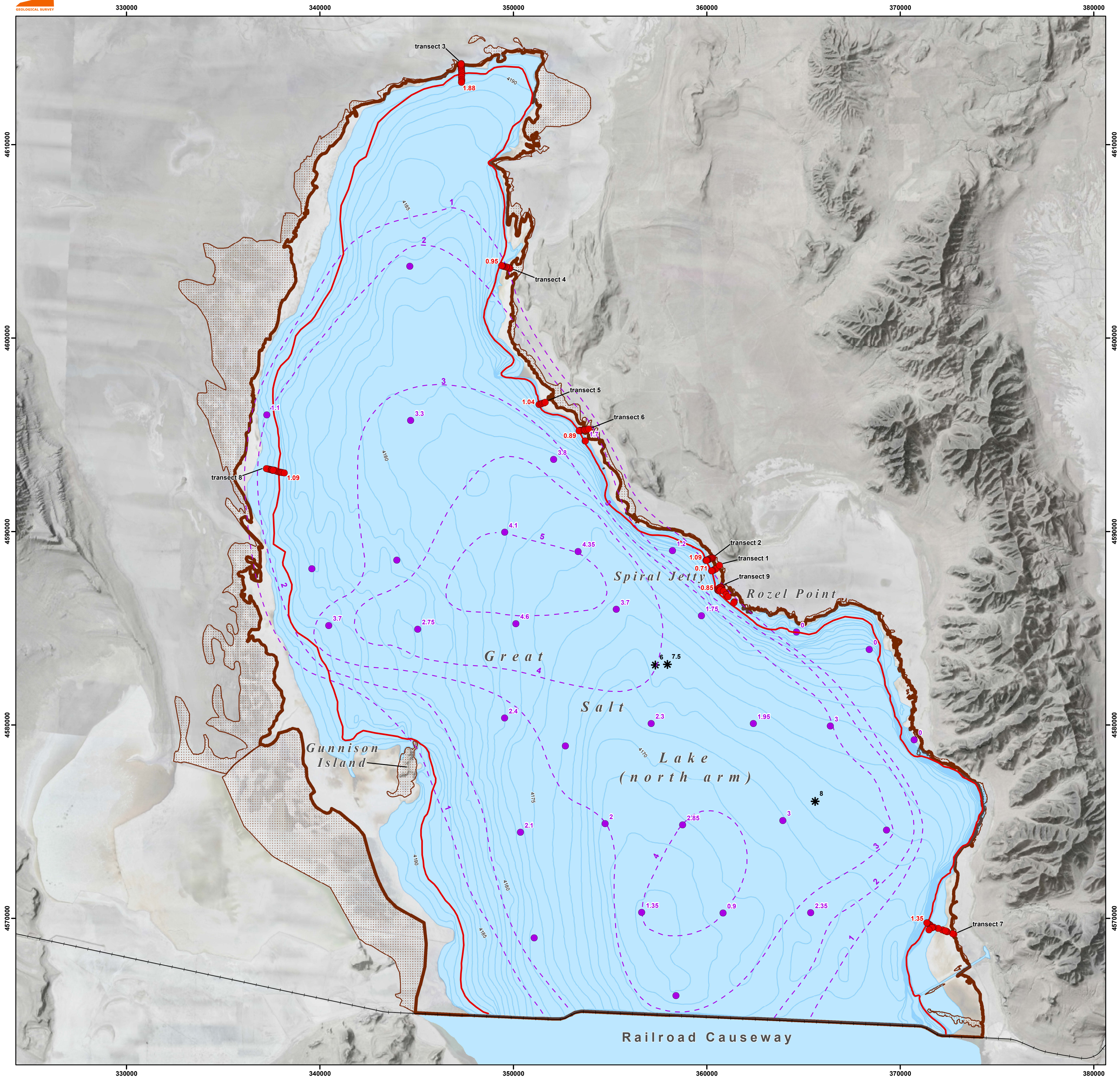
Sample No.	Th Soluble ppm	TiO₂ Soluble wt. %	U Soluble ppm	V Soluble ppm	W Soluble ppm	Y Soluble ppm	Yb Soluble ppm	Zn Soluble ppm
SCI 1.2	<1	<0.01	<2	<1	<1	<1	<0.1	<1
SCI 1.4	<1	<0.01	<2	<1	<1	<1	<0.1	<1
SCI 2.2	<1	<0.01	<2	<1	<1	<1	<0.1	<1
SCI 2.4	<1	<0.01	<2	<1	<1	<1	<0.1	<1
SCI 3	<1	<0.01	<2	<1	<1	<1	<0.1	<1
SCI 3 R	<1	<0.01	<2	<1	<1	<1	<0.1	<1

Sample No.	Zr Soluble ppm	Insolubles wt. %	Moisture wt. %
SCI 1.2	<1	0.3	0.2
SCI 1.4	<1	0.2	0.3
SCI 2.2	<1	0.2	0.4
SCI 2.4	<1	0.1	0.3
SCI 3	<1	0.1	0.1
SCI 3 R	<1	0.1	0.1

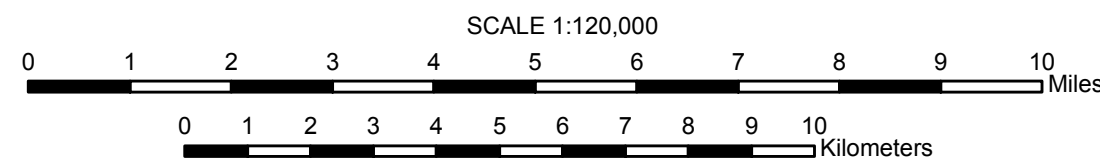
Appendix D Salt Crust Thickness Measurement Data

Station	Transect Number	Thickness Average (ft)	Thickness Average (inches)	Thickness 1 (inches)	Thickness 2 (inches)	Thickness 3 (inches)	Thickness 4 (inches)	Standard Deviation (inches)	Standard Deviation (ft)	UTM Z12 NAD83		Date Measured	Measurement in water?	Number of holes used for measurement	Comment	
										UTM Easting (m)	UTM Northing (m)					
GIS Headers:	station	transect	thk avg ft	thk avg in	thk 1 in	thk 2 in	thk 3 in	thk 4 in	stddev in	stddev ft	utm 83	utm 83	date	water	no holes	comment
8	1	0.71	8.47	8.500	8.500	8.500	8.375	0.06	0.005	360262	4587971	13-Aug-15	yes	3		
9	1	0.55	6.58	6.625	6.625	6.500		0.07	0.006	360301	4587988	13-Aug-15	no	3		
10	1	0.33	3.96	4.000	4.000	3.875		0.07	0.006	360333	4588001	13-Aug-15	no	3		
11	1	0.25	3.00	3.000	3.000	3.000		0.00	0.000	360380	4588026	13-Aug-15	no	3?		
12	1	0.25	3.00	2.625	3.250	3.125		0.33	0.028	360422	4588044	13-Aug-15	no	3?		
13	1	0.09	1.08	1.000	1.000	1.250		0.14	0.012	360465	4588064	13-Aug-15	no	3?		
15	1	0.00	0.00	0.000						360660	4588249	13-Aug-15	no	n/a	edge of salt crust	
16	2	0.00	0.00	0.000						360305	4588631	21-Aug-15	no	n/a	edge of salt crust; patchy to east	
17	2	0.13	1.56	1.625	1.625	1.500	1.500	0.07	0.006	360262	4588631	21-Aug-15	no	2		
18	2	0.17	2.00	2.000	2.000	2.000	2.000	0.00	0.000	360220	4588612	21-Aug-15	no	2		
19	2	0.13	1.59	1.625	1.625	1.500	1.625	0.06	0.005	360168	4588596	21-Aug-15	no	2		
20	2	0.26	3.16	3.000	3.000	3.500	3.125	0.24	0.020	360110	4588563	21-Aug-15	no	2		
21	2	0.35	4.16	4.250	4.000	4.250	4.125	0.12	0.010	360062	4588545	21-Aug-15	no	2		
22	2	0.52	6.25	6.250	6.250	6.000	6.500	0.20	0.017	360031	4588534	21-Aug-15	no	2		
23	2	0.68	8.16	8.125	8.375	8.125	8.000	0.16	0.013	359999	4588525	21-Aug-15	no	2	sample SCI-1 collected	
24	2	1.09	13.06	13.000	13.125	13.000	13.125	0.07	0.006	359982	4588516	21-Aug-15	yes	2		
26	3	0.93	11.22	11.125	11.250	11.250	11.250	0.06	0.005	347309	4614055	25-Aug-15	no	2		
27	3	1.08	12.91	12.625	13.250	12.750	13.000	0.28	0.023	347310	4614016	25-Aug-15	no	2		
28	3	1.04	12.53	13.125	13.000	12.000	12.000	0.62	0.051	347311	4613967	25-Aug-15	no	2		
29	3	1.10	13.16	13.000	13.625	12.875	13.125	0.33	0.027	347317	4613918	25-Aug-15	no	2		
30	3	1.12	13.44	12.750	13.750	14.000	13.250	0.55	0.046	347321	4613847	25-Aug-15	no	2	may be about 1.5 inches of salt below about 2 inches of mud bed below the top salt	
31	3	0.69	8.28	7.750	8.500	8.375	8.500	0.36	0.030	347325	4613768	25-Aug-15	no	2	probed for deeper salt, but none encountered	
32	3	0.94	11.25	11.000	11.500			0.35	0.029	347326	4613696	25-Aug-15	no	1		
33	3	1.31	15.75	15.750	15.750			0.00	0.000	347331	4613589	25-Aug-15	yes	1	possible small zone of mud (less than an inch?)	
34	3	1.58	19.00	19.000	19.000			0.00	0.000	347324	4613492	25-Aug-15	yes	1	possible small zone of mud (less than an inch?)	
35	3	1.68	20.19	19.875	20.500			0.44	0.037	347328	4613373	25-Aug-15	yes	1	possible small zone of mud (less than an inch?)	
36	3	1.58	18.94	19.000	18.875			0.09	0.007	347328	4613287	25-Aug-15	yes	1		
37	3	1.88	22.50	22.125	23.000	22.375	22.500	0.37	0.031	347324	4613216	25-Aug-15	yes	2		
38	3	0.66	7.88	8.750	7.750	7.500	7.500	0.60	0.050	347301	4614104	25-Aug-15	no	2	may be a few inches of additional salt below top salt; measurements represent top salt	
39	3	0.00	0	0.000						347305	4614193	25-Aug-15	no	n/a		
40	3	0.21	2.5	2.500	2.500			0.00	0.000	347301	4614160	25-Aug-15	no	1		
41	4	0.00	0	0.000						349822	4603612	31-Aug-15	no	n/a	linear microbialite mound/reef?	
42	4	0.30	3.56	3.750	3.625	3.625	3.250	0.22	0.018	349795	4603627	31-Aug-15	no	2		
43	4	0.30	3.56	3.500	3.625			0.09	0.007	349734	4603653	31-Aug-15	no	1		
44	4	0.26	3.13	3.000	3.250			0.18	0.015	349655	4603673	31-Aug-15	no	1		
45	4	0.59	7.13	7.125	7.125			0.00	0.000	349623	4603680	31-Aug-15	no	1	measurement from a mound	
46	4	0.41	4.88	5.000	4.750	4.875		0.13	0.010	349530	4603701	31-Aug-15	no	1		
47	4	0.43	5.19	5.250	5.125			0.09	0.007	349474	4603720	31-Aug-15	no	1		
48	4	0.86	10.31	10.000	10.625			0.44	0.037	349436	4603735	31-Aug-15	no	2	a soft zone of forming or dissolving (?) crust is not represented in this measurement (maybe an inch?)	
49	4	0.95	11.38	11.250	11.500			0.18	0.015	349423	4603742	31-Aug-15	yes	1		
50	4	0.95	11.44	11.125	11.750			0.44	0.037	349398	4603755	31-Aug-15	yes	1	edge of mound; possible error introduced by bioherm	
51	4	0.92	11.06	10.625	11.500			0.62	0.052	349402	4603751	31-Aug-15	yes	1	possible small zone of mud (less than an inch?)	
52	5	0.39	4.69	4.625	4.750			0.09	0.007	351423	4596603	31-Aug-15	no	1		
53	5	0.61	7.31	7.375	7.250			0.09	0.007	351370	4596580	31-Aug-15	no	1		
54	5	0.94	11.25	11.000	11.500			0.35	0.029	351344	4596573	31-Aug-15	yes	1		
55	5	0.97	11.69	11.750	11.625			0.09	0.007	351334	4596571	31-Aug-15	yes	1		
56	5	1.04	12.44	12.125	12.750			0.44	0.037	351329	4596568	31-Aug-15	yes	1		
57	5	0.36	4.38	4.375	4.375			0.00	0.000	351442	4596608	31-Aug-15	no	1	salt crust covered by thin veneer of oolitic mud	
58	5	0.23	2.81	2.750	2.875			0.09	0.007	351514	4596628	31-Aug-15	no	1	salt crust covered by thin veneer of oolitic mud	
59	5	0.25	3.00	2.875	3.125			0.18	0.015	351598	4596659	31-Aug-15	no	1	salt crust covered by thin veneer of oolitic mud	
60	5	0.21	2.50	2.625	2.375			0.18	0.015	351652	4596685	31-Aug-15	no	1	salt crust patchy to NE of this location	
61	6	0.23	2.75	2.750	2.750			0.00	0.000	353566	4595239	2-Sep-15	no	1		
62	6	0.29	3.44	3.375	3.500			0.09	0.007	353511	4595229	2-Sep-15	no	1		
63	6	0.34	4.06	3.875	4.250			0.27	0.022	353465	4595233	2-Sep-15	no	1		
64	6	0.67	8.00	7.875	8.125			0.18	0.015	353430	4595221	2-Sep-15	?	1		
65	6	0.82	9.81	10.000	9.625			0.27	0.022	353411	4595215	2-Sep-15	yes	1		
66	6	0.89	10.69	10.375	11.000			0.44	0.037	353405	4595209	2-Sep-15	yes	1		
67	n/a	0.56	6.75	6.500	6.875	7.000	6.625	0.23	0.019	353720	4594675	2-Sep-15	no	2		
68	6	0.22	2.63	2.500	2.750			0.18	0.015	353658	4595252	2-Sep-15	no	1		
69	6	0.17	2.00	2.000	2.000			0.00	0.000	353712	4595255	2-Sep-15	no	1		
70	6	0.10	1.19	1.250	1.125			0.09	0.007	353815	4595276	2-Sep-15	no	1		
71	6	0.00	0.00	0.000						353897	4595294	2-Sep-15	no	n/a	transitional area	
72	7	0.10	1.25	1.250						372769	4569186	9-Sep-15	no	n/a	bioherm area, salt between bioherms	

Station	Transect Number	Thickness Average (ft)	Thickness Average (inches)	Thickness 1 (inches)	Thickness 2 (inches)	Thickness 3 (inches)	Thickness 4 (inches)	Standard Deviation (inches)	Standard Deviation (ft)	UTM Z12 NAD83		Date Measured	Measurement in water?	Number of holes used for measurement	Comment
										UTM Easting (m)	UTM Northing (m)				
GIS Headers:															
station	transect	thk avg ft	thk avg in	thk 1 in	thk 2 in	thk 3 in	thk 4 in	stddev in	stddev ft	utm_e 83	utm_n 83	date	water	no holes	comment
73	7	0.10	1.25	1.000	1.500			0.35	0.029	372708	4569209	9-Sep-15	no	n/a	bioherm area, salt between bioherms
75	7	0.63	7.50	7.125	7.375	7.875	7.625	0.32	0.027	372431	4569312	9-Sep-15	no	2	bioherm area, base of salt difficult to distinguish
76	7	0.78	9.42	8.500	10.750	9.000		1.18	0.098	372297	4569365	9-Sep-15	no	1	bioherm area, base of salt difficult to distinguish
77	7	0.75	9.03	9.750	9.500	8.875	8.000	0.78	0.065	372176	4569409	9-Sep-15	no	2	bioherm area, base of salt difficult to distinguish, possible mud zone
78	7	0.95	11.38	12.000	12.375	10.250	10.875	0.98	0.082	371958	4569486	9-Sep-15	no	2	bioherm area, base of salt difficult to distinguish, possible mud zone
80	7	0.58	7.00	7.000						371546	4569664	9-Sep-15	no	2	bioherm area; this site was excavated for a confident thickness; sample SCI-2 collected
81	7	1.20	14.38	14.250	14.500			0.18	0.015	371475	4569711	9-Sep-15	yes	1	bioherm area, base of salt difficult to distinguish
82	7	0.82	9.78	9.625	9.875	9.750	9.875	0.12	0.010	371424	4569738	9-Sep-15	yes	2	bioherm area, base of salt difficult to distinguish
83	7	1.35	16.25	15.750	16.750			0.71	0.059	371388	4569765	9-Sep-15	yes	1	bioherm area, base of salt difficult to distinguish
84	7	1.08	12.94	12.125	13.750			1.15	0.096	371376	4569774	9-Sep-15	yes	1	bioherm area, base of salt difficult to distinguish
85	n/a	0.58	7.00	7.000						372392	4569326	23-Sep-15	no	n/a	bioherm area, measured in dissolution hole, minimum thickness (?)
86	n/a	0.69	8.25	8.250						372328	4569354	23-Sep-15	no	n/a	bioherm area, measured in dissolution hole, minimum thickness (?)
87	n/a	0.50	6.00	4.500	6.500	7.000		1.32	0.110	371723	4569550	23-Sep-15	no	3	bioherm area, measured from a few holes within a few meters, measured by cuttings change
88	n/a	0.42	5.04	3.750	4.875	6.500		1.38	0.115	371656	4569519	23-Sep-15	no	3?	bioherm area, measured from a few holes within a few meters, measured by cuttings change
89	n/a	0.54	6.50	6.500						371648	4569519	23-Sep-15	no	n/a	bioherm area, measured in dissolution hole, minimum thickness (?)
90	n/a	0.61	7.38	7.375						371482	4569420	23-Sep-15	no	1	bioherm area, measured by cuttings change
91	8	0.61	7.29	7.125	7.250	7.500		0.19	0.016	337439	4593204	30-Sep-15	no	1	
92	8	0.53	6.38	6.125	5.875	7.125		0.66	0.055	337423	4593209	30-Sep-15	no	1	
93	8	0.51	6.13	6.250	6.125	6.000		0.13	0.010	337364	4593229	30-Sep-15	no	1	
94	8	0.38	4.54	4.750	4.375	4.500		0.19	0.016	337308	4593243	30-Sep-15	no	1	
95	8	0.60	7.17	7.125	7.125	7.250		0.07	0.006	337234	4593264	30-Sep-15	no	2?	one measurement from cuttings change
96	8	0.58	6.94	7.500	6.375			0.80	0.066	337494	4593189	30-Sep-15	no	?	possibly bioherm area
97	8	0.57	6.81	7.000	6.625			0.27	0.022	337507	4593182	30-Sep-15	no	1	
98	8	0.68	8.17	7.750	8.375	8.375		0.36	0.030	337570	4593164	30-Sep-15	no	1	
99	8	0.94	11.31	11.250	11.375			0.09	0.007	337603	4593173	30-Sep-15	yes	1	
100	8	0.88	10.50	10.250	10.750			0.35	0.029	337626	4593171	30-Sep-15	yes	1	
101	8	0.95	11.38	11.125	11.375	11.625		0.25	0.021	337691	4593163	30-Sep-15	yes	1	
102	8	0.86	10.33	10.250	10.500	10.250		0.14	0.012	337780	4593118	30-Sep-15	yes	1	
103	8	1.06	12.67	12.750	12.500	12.750		0.14	0.012	337894	4593079	30-Sep-15	yes	1	
104	8	1.09	13.13	13.250	13.125	13.000		0.13	0.010	337945	4593071	30-Sep-15	yes	1	
105	8	1.01	12.13	12.000	12.250			0.18	0.015	337997	4593063	30-Sep-15	yes	1	
106	8	1.01	12.13	12.000	12.250			0.18	0.015	338057	4593051	30-Sep-15	yes	1	
107	8	1.06	12.75	12.750	12.750			0.00	0.000	338160	4593041	30-Sep-15	yes	1	
108	8	0.67	8.00	8.000						337577	4593173	30-Sep-15	no	n/a	coordinate is estimated; sample SCI-3 collected; excavation for thickness measurement
109	9	0.00	0.00	0.000						360748	4587135	13-Nov-15	no	n/a	
110	9	0.68	8.19	8.125	8.250			0.09	0.007	360724	4587129	13-Nov-15	no	1	
111	9	0.55	6.56	6.500	6.625			0.09	0.007	360694	4587117	13-Nov-15	no	1	
112	9	0.63	7.50	7.500	7.500			0.00	0.000	360649	4587092	13-Nov-15	no	1	
113	9	0.61	7.31	7.250	7.375			0.09	0.007	360615	4587066	13-Nov-15	yes	1	
114	9	0.77	9.25	8.750	9.375	9.625		0.45	0.038	360570	4587038	13-Nov-15	yes	1	
116	9	0.80	9.63	10.250	9.375	9.250		0.54	0.045	360570	4586976	13-Nov-15	yes	1	
117	9	0.82	9.81	9.625	10.000			0.27	0.022	360589	4586965	13-Nov-15	yes	1	
118	9	0.85	10.19	10.125	10.250			0.09	0.007	360626	4586934	13-Nov-15	yes	1	
119	9	0.82	9.81	9.875	9.750			0.09	0.007	360657	4586936	13-Nov-15	yes	1	
120	9	0.72	8.69	8.625	8.750			0.09	0.007	360698	4586982	13-Nov-15	yes	1	
121	9	0.61	7.38	7.500	7.250			0.18	0.015	360865	4586920	13-Nov-15	no	1	
122	9	0.57	6.81	6.750	6.875			0.09	0.007	360996	4586751	13-Nov-15	no	1	
123	9	0.59	7.13	7.125	7.125			0.00	0.000	361096	4586637	13-Nov-15	no	1	
124	9	0.53	6.31	6.500	6.125			0.27	0.022	361417	4586360	13-Nov-15	no	1	
125	9	0.71	8.56	8.500	8.625			0.09	0.007	361399	4586317	13-Nov-15	yes	1	
16	2	0.00	0.00	0.000						360305	4588631	4-Mar-16	no	n/a	
17	2	0.00	0.00	0.000						360262	4588631	4-Mar-16	no	n/a	patches of crust in this area
18	2	0.15	1.83	1.750	2.000	1.750		0.14	0.012	360220	4588612	4-Mar-16	no	1	
19	2	0.08	0.97	1.000	0.875	1.000	1.000	0.06	0.005	360168	4588596	4-Mar-16	no	2	
20	2	0.25	3.04	3.000	3.000	3.125		0.07	0.006	360110	4588563	4-Mar-16	no	1	
21	2	0.25	2.96	3.125	2.875	2.875		0.14	0.012	360062	4588545	4-Mar-16	no	1	
22	2	0.43	5.13	5.250	5.125	5.000		0.13	0.010	360031	4588534	4-Mar-16	no	1	found previous hole, but measured a new hole
23	2	0.58	6.96	6.750	7.000	7.125		0.19	0.016	359999	4588525	4-Mar-16	no	1	
24	2	0.84	10.13	10.250	10.375	9.750		0.33	0.028	359982	4588516	4-Mar-16	yes	1	
126	2	0.91	10.94	10.875	11.000			0.09	0.007	359958	4588510	4-Mar-16	yes	1	
22	2	0.42	5.00	5.000	5.000			0.00	0.000	360031	4588534	7-Apr-16	no	1	found previous hole, but measured a new hole
23	2	0.54	6.50	6.625	6.375			0.18	0.015	359999	4588525	7-Apr-16	no	1	found previous hole, but measured a new hole
24	2	0.66	7.97	7.750	7.875	8.375	7.875	0.28	0.023	359982	4588516	7-Apr-16	yes	2	found previous hole, used both old and new holes
8	1	0.25	2.96	2.750	3.000	3.125		0.19	0.016	360262	4587971	7-Apr-16	yes	1	only a few inches from shore
9	1	0.41	4.94	5.000	4.875			0.09	0.007	360301	4587988	7-Apr-16	no	1	
127	1	0.65	7.81	7.500	8.125			0.44	0.037	360250	4587966	7-Apr-16	yes	1	



Although this product represents the work of professional scientists, the Utah Department of Natural Resources, Utah Geological Survey, makes no warranty, expressed or implied, regarding its suitability for a particular use, and does not guarantee accuracy or completeness of the data. The Utah Department of Natural Resources, Utah Geological Survey, shall not be liable under any circumstances for any direct, indirect, special, incidental, or consequential damages with respect to claims by users of this product.



Base from Utah hillshade 10-meter elevation provided by AGRC (2016)
 Projection: UTM, Zone 12N
 Units: Meters
 Datum: NAD 1983
 Utah Geological Survey
 1594 West North Temple, Suite 3110
 P.O. Box 146100, Salt Lake City, UT 84114-6100
 (801) 537-3300
geology.utah.gov

NORTH ARM SALT CRUST MAP AND THICKNESS DATA

by
 Andrew Rupke, Taylor Boden, and Peter Nielsen
 2016

EXPLANATION

- UGS transect data point (maximum salt thickness in feet)
- UGS 1-foot salt isopach (late 2015)
- Goodwin (1973a) data point (salt thickness in feet) (some holes did not completely penetrate salt crust)
- - - Goodwin (1973a) salt isopach (feet)
- * 1974 Amoco borehole (Dames and Moore, undated) (salt thickness in feet)
- Salt crust partial area (2014)
- Salt crust area (2014)
- 1-foot bathymetric contour (Baskin and Turner, 2006)
Elevation of lake bottom in feet above mean sea level